Microstrip Patch Antenna with Dual Equilateral Triangular Cut Resonators Structure for WLAN Application

by

Sunanda Roy

A thesis submitted in partial fulfillment of the requirements for the degree of Master of Engineering in Electrical and Electronic Engineering

Electrical and Electronic Engineering Department
Khulna University of Engineering & Technology (KUET)
Khulna-9203, Bangladesh

February, 2016

Declaration

This is to certify that the thesis work entitled as, "*Microstrip Patch Antenna with Dual Equilateral Triangular Cut Resonators Structure for WLAN Application*", has been carried out by *Sunanda Roy* in the Department of *Electrical and Electronic Engineering*, Khulna University of Engineering & Technology (KUET), Khulna, Bangladesh. The above thesis work or any part of this work has not been submitted anywhere for the award of any degree or diploma.

..... **.....**

Signature of Supervisor Signature of Candidate

Dedicated to My Parents

Sushanta Roy & Bashanti Roy

Those who have chosen underprivileged life to continue my smile.

ACKNOWLEDGEMENTS

Time is like a fleeting show. Three years of M.Sc. Engineering degree with research may be the most important period in my life. The research result of the M.Sc. is not only several academic papers, but most importantly, the way how I am thinking and acting in the academic field, which will definitely change my career in the future.

Firstly, I owe an endless gratitude to my supervisor Dr. M. Abdus Samad Professor, Electrical and Electronic Engineering Department, Khulna University of Engineering and Technology for the opportunity of working under him. He had helped me at each and every point of the thesis work with his dedication, comments, suggestions and guidance which put me on the right path to fulfill the requirement, without which this situation was impossible to overcome. I learnt a lot of things from him, not only the academic knowledge, but also the way of research. This will be precious wealth in all my future academic life. Our communication is always flexible and efficient. That is the main reason why we can achieve so many publications. He also friendly supported me a lot in my daily life which I am truly appreciated.

I am also so much grateful to Dr. Md. Nurunnabi Mollah, the honourable professor, Faculty of Electrical and Electronic Engineering, KUET, as well as the member of this thesis examination committee, for his loving and cordial advices to prepare my thesis proposal and final thesis paper.

My deep thanks also go to respective teacher Professor Dr. Ashraful G. Bhuiyan, Head of Electrical and Electronic Engineering Department, Khulna University of Engineering & Technology, Khulna, for his precious implication.

Besides, I am eternally grateful to my M.Sc. thesis committee member, Professor Dr. Mohammad Shaifur Rahman. He also gave me a lot of suggestions and comments in my report that help improve the thesis a lot. I also wish to express my sincere appreciation for his valuable time and advices.

And last but not the least to express my heartiest thanks to GOD and all of those who supported us directly or indirectly to complete the task.

Sunanda Roy
February, 2016
KUET, Khulna

TABLE OF CONTENTS

LIST OF FIGURES

LIST OF TABLE

LIST OF ACRONYMS

ADS	Advance Design System
BW	Bandwidth
CPW	Coplanar Waveguide
CST	Computer Simulation Technology
CTCSRR	complementary triangular cut split-ring resonator
CTCSRRs	complementary triangular cut split-ring resonators
DETCSRR	Dual Equilateral Triangular Cut Split Ring Resonator
EM	Electro Magnetic
ETCSRR	Equilateral Triangular Cut Split Ring Resonator
MICs	Microwave integrated circuits
RF	Radio Frequency
RL	Return Loss
SRR	Split Ring Resonator
TEM	Transverse-electric-magnetic
T-SRR	Triangular Split Ring Resonator
VSWR	Voltage Standing Wave Ratio
WLAN	Wireless Local Area Network

ABSTRACT

The necessity for wireless communication and its esoteric nature is enlarging during the two decades. In future, it is deduced to be more challenging and elaborate with evolution of different types of patch antenna with different structures. Nowadays, smaller size of electronic equipment demand same size antenna element in order to place properly in the wireless devices without changing the radiation properties of antenna. Antenna plays an important role in WLAN communication system because it performance depend upon the quality of wireless communication. Providing of a quality service for the recently increased demand in WLAN is a core level concern as usually for antenna and communication devices. The WLAN is used in our everyday life applications such as notebooks, mobile phones, routers etc. To meet the daily increasing needs, antennas used in WLAN applications are noteworthy factor. With respect to performance, a low cost feed network with miniaturization in size is also very important to carry out in terms of antenna design. This thesis work focuses mostly on design and analysis of microstrip patch antenna using split ring resonator structure as well as effects of triangular cut resonator structure made on patch antenna to improve the return loss, gain and directivity. We present characteristics of microstrip patch antennas on Roger RT/Duroid 5880 substrates loaded with complementary equilateral triangular cut split-ring resonators (CETCSRRs) and study the various effects of design parameters like size of resonator, number of resonator, location of resonator and orientation between two resonators for WLAN applications. The proposed antennas are designed using CST 2014 microwave studio. The simulated results represent that the CTCSRR loaded patch antenna achieves better performance in terms of gain, directivity and return loss. The radiation properties of a rectangular patch antenna with triangular split ring resonator structure designed on Roger RT/Duroid 5880 substrate are obtained and compared with that of a normal rectangular patch antenna designed under same criteria.

CHAPTER 1

INTRODUCTION

1.1 Overview

An explosive growth of the wireless radio communication systems is currently observed in the microwave band. In the short range communications or contactless identification systems, single band antenna has been playing a very important role for wireless service requirements [1]. Wireless local area network (WLAN) has been widely applied in mobile devices such as handheld computers and intelligent phones. This technique has been widely considered as a cost effective, viable and high speed data connectivity solution, enabling user mobility [2].Microstrip patch antennas [3], are popular in wireless communication, because they have some advantages due to their conformal and simple planar structure. They allow all the advantages of printed -circuit technology. There are varieties of patch structures available but the rectangular, circular and triangular shapes [3], are most frequently used. Design of WLAN antennas also got popularity with the advancement of microstrip antennas.

Moreover a large number of microstrip patches to be used in wireless applications have been developed [4] . The rapid progress in wireless communications requires the development of lightweight, low profile, single feed antennas. Also it is highly desirable to integrate several RF modules for different frequencies into one piece of equipment. Hence, WLAN antennas that can be used simultaneously in different standards have been in the focus points of many research projects [5]. Portable devices are widely used in our daily lives such as mobile phones, laptops with wireless connection [6].

The main goal of this work is to improve the performance of the antenna very effectively and for Triangular split ring resonator and dual triangular split ring resonator structure were introduced to the conventional antenna. This work achieves better performance in comparison to simpler structure. The proposed antenna structure in this work can be used for WLAN applications.

The first design of simple rectangular microstrip patch antenna, secondly design is to develop with single complementary triangular split ring resonator and dual complementary triangular split ring resonator this simple antenna at 2.44GHz for WLAN application.

Last but not least, computer simulation software, CST will be used to design and simulate the antenna. The CST is capable to generate antenna design simulation faster compared to Microwave Office and be able to draw a 3-D antenna configuration.

1.2 Problem Statement

In recent years, demand for small antennas on wireless communication has increased the interest of research work on compact microstrip antenna design among microwave and wireless engineers [7].With the rapid growth of wireless communication as well as WLAN, the increasing popularity of cellular system is prompting the development of efficient antennas. Antenna is the critical device or equipment that is used to efficiently transmit wireless signal to the free space and/or receive wireless signal [1].

In the last few years, the wireless communications industry has grown by orders of magnitude fueled by digital and RF circuit fabrication improvements, new large-scale circuit integration, and other miniaturization technologies which make portable radio equipment smaller, cheaper, and more reliable. Patch antenna can provide those requirements due to its size is very small, low profile, light weight compared to other conventional mobile antennas. Among all the advantages, there are few drawbacks of using patch antenna which are low gain, low return loss, narrow bandwidth, high ohmic losses and low efficiency. However, in order to achieve those antenna characteristics which is suitable for WLAN applications; it is proposed to introduce equilateral triangular cut resonator structure at the top of the patch of microstrip patch antenna. The advantages of this resonator structure compared to other split ring resonator (i.e. rhombic, circular, and elliptical) are simple in designing and make the antenna compact. But some antenna characteristics will be degraded by using this technique. Therefore, in order to further improve the antenna performance another technique is proposed which is by loading a dual equilateral triangular cut resonator structure at the top of the patch of microstrip patch antenna. Hence, at the

end of the project it's expected to achieve single equilateral triangular cut resonator structure and dual equilateral triangular cut resonator structure antenna with improved performance.

1.3 Objectives of Thesis

- The objectives of this project are:
- Studying the rectangular probe feed patch antenna with different types of Split ring resonators.
- Proposing a patch antenna configuring rectangular geometry incorporated with single triangular resonator shape as well as dual triangular cut resonator structure.
- Selecting substrate and materials for proposed DETCR structure on microstrip patch antenna.
- Analyzing the obtained result on the basis of different criteria (i.e. size variation, distance between structures, number of resonators, and orientation of resonators).
- Analyzing and comparing performance parameters in obtained results with conventional patch antenna.
- Validification of the expected improved performance will be discussed.

1.4 Motivation of Thesis

Use of conventional microstrip antenna is limited because of their poor gain, low return loss, low directivity, low bandwidth and polarization purity. There has been a lot of research in the past decade in this area.

The proposed techniques inclusion of single and dual cut resonator develops stored capacitive charge and boosts the antenna radiation and electromagnetic field which enhances the antenna performance. The probe feeding techniques are also extensively helped to improve these performances with designed structure.

This work is primarily focused on designing of ETCSRR and DETCSRR structure for improving the antenna performances which will be better than conventional microstrip antenna. The designed structure with microstrip patch antenna has become efficient for WLAN applications in wireless communication area.

1.5 The Scopes of The thesis

This work focuses following major components to fulfill the objectives of the thesis, which represent as below:

- The frequency operation of this compact antenna is from 2.4GHz to 2.44GHz, which is the WLAN application frequency ranges. Also the resonant frequency of the conventional antenna is selected as 2.4 GHz.
- Antenna characteristics such as S11, gain, directivity, radiation efficiency, radiation pattern and 3 dB beam width will be discussed in this work.
- The antenna will be simulated by using CST microwave studio. This software is chosen because it is a specialist tool for the 3D EM simulation of high frequency components.
- The velidefication of proposed structure clearly established.
- Result analysis of radiation pattern will be limited to simulation measurement only.

1.6 Thesis Outline

This thesis is divided into 4 main chapters and the reference section.
Chapter 1 discusses about the introduction, problem statement, objectives and scope of the project.

Chapter 2 briefs literature studies of the microstrip antenna in order to get its basic fundamental. The main aspects of the microstrip antenna such as its structure configuration, radiation mechanism, polarization, feeding techniques, method of analysis etc are covered. Previous researches related with the project also presented in this chapter.

Chapter 3 describes the design procedure of single band, and triple band Rectangular Microstrip patch antenna using coaxial feeding technique. The designing and simulation using CST Microwave Studio of rectangular microstrip patch antenna is done and simulation results are presented, the fabrication procedure of the antenna and various instruments used for antenna fabrication. The snap shots of the fabricated antenna are also given in this chapter. This chapter

also describes some techniques to improve the compactness off the microstrip patch antenna using SRR.

Chapter 4 analysis the results of the proposed antenna such as return loss (dB), radiation pattern, gain and radiation efficiency. Also the comparison of the simulated and measured results is presented in this chapter.

Chapter 5 represents the velidefication of proposed structure. Here compares the performance parameter between the complete antenna structure and its equivalent circuit.

Chapter 6 gives the conclusion to this thesis and the future work continued antenna design by using a different structure configuration.

CHAPTER 2

Antenna Fundamentals

In this chapter, the basic concept of an antenna, antenna definition, its origin and its working has been explained. Next, some performance parameters of antenna have also been discussed.

2.1 Introduction to Antenna

Antennas are structures used to collect or radiate electromagnetic waves. It can be considered as specialized transducers that can convert RF fields into AC line signals or vice versa. According to Webster's Dictionary, antenna is defined as "a usually metallic device (as a rod or wire) for radiating or receiving radio waves". According to The IEEE Standard Definitions (IEEE Std 145–1983), antenna or aerial is "a means for radiating or receiving radio waves" [8].

2.2 Types of Antenna

The two main types of antennas are the receiving antenna, which intercepts RF energy and delivers AC signals to electronic equipment, and the transmitting antenna, which is fed with AC signals from electronic equipment and generates an RF field. Some of the commonly used antennas are half-wave dipole antennas, monopole antennas, helical antennas, horn antennas etc. Antenna has many uses; communication, radar, telemetry, navigation etc [8].

2.3 How an Antenna Radiates

In order to know how an antenna radiates, let us first consider how radiation occurs. A conducting wire radiates mainly because of time-varying current or acceleration (or deceleration) of charge. The conditions of radiation are [8]

1. If there is no motion of charges in a wire, no radiation takes place, since no flow of current occurs.
2. If charges are moving with uniform velocity
    a) Radiation will not occur if the wire is straight.
    b) Charges moving with uniform velocity will produce radiation if the wire is curved, bent, discontinuous, terminated or truncated.
3. If charge is oscillating in a time-motion, it radiates even if the wire is straight.

If the charge is oscillating with time, then radiation occurs even along a straight wire [8]. The radiation from an antenna can be explained with the help of figure 2.1 which shows a voltage source connected to a two conductor transmission line. When a sinusoidal voltage is applied across the transmission line, an electric field is created which is sinusoidal in nature and this result in the creation of electric lines of force which are tangential to the electric field. The free electrons on the conductors are forcibly displaced by the electric lines of force and the movement of these charges causes the flow of current which in turn leads to the creation of a magnetic field.

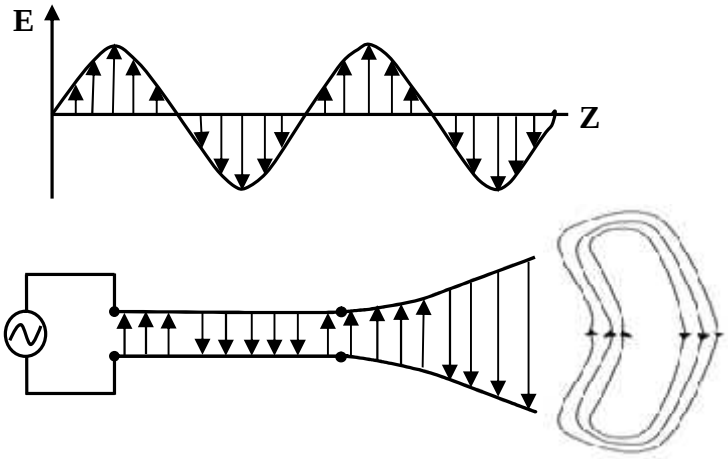

Figure 2.1: Radiations from an Antenna.

Due to the time varying electric and magnetic fields, electromagnetic waves are created and these travel between the conductors. As these waves approach open space, free space waves are formed by connecting the open ends of the electric lines. Since the sinusoidal source continuously creates the electric disturbance, electromagnetic waves are created continuously and these travel through the antenna and are radiated into the free pace. Inside the transmission line and the antenna, the electromagnetic waves are sustained due to the charges, but as soon as

they enter the free space, they form closed loops and are radiated. The field patterns, associated with an antenna, change with distance and are associated with two types of energy, radiating energy and reactive energy. Hence, the space surrounding an antenna can be divided into three regions as shown in figure 2.2 [8].

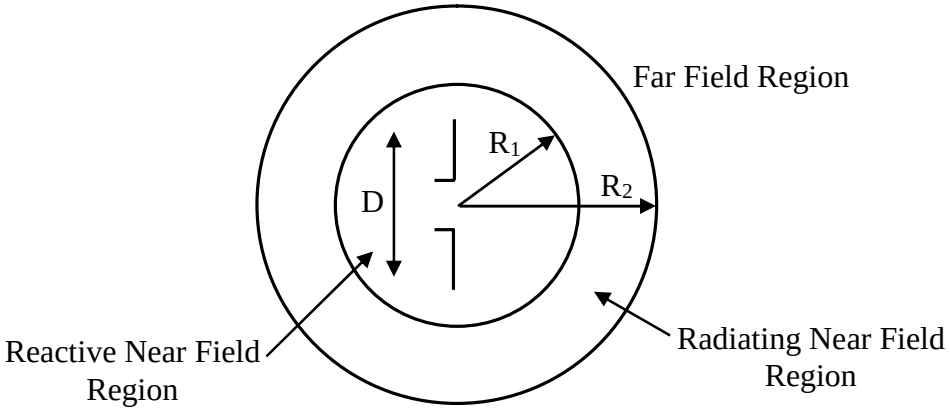

Figure 2.2: Field regions around an antenna.

2.3.1 Reactive Near Field Region

Reactive near field region is defined as that portion of the near field region immediately surrounding the antenna where the reactive field pre-dominates [8].

2.3.2 Radiating Near Field Region

Radiating near field region is that region of the field of an antenna between the reactive near field region and far field region where in the radiation field pre-dominates [8].

2.3.3 Far Field Region

Far field region is that region where the angular field distribution is essentially independent of the distance from the antenna [8].

2.4 Antenna Performance Parameters

An antenna is a device that is made to radiate and receive electromagnetic waves efficiently. There are several important antenna parameters that should be considered when choosing an antenna for application which are as follows;

2.4.1 Input Impedance

The input impedance of an antenna is defined by as “the impedance presented by an antenna at its terminals or the ratio of the voltage to the current at the pair of terminals or the ratio of the appropriate components of the electric to magnetic fields at a point”. Hence the impedance of the antenna can be written as [9],

$$Z_{in} = R_{in} + jX_{in} \tag{2.1}$$

Where

Z_{in} = Antenna impedance at the terminals

R_{in} = Antenna resistance at the terminals

X_{in} = Antenna reactance at the terminals

The imaginary part, X_{in} of the input impedance represents the power stored in the near field of the antenna. The resistive part, R_{in} of the input impedance consists of two components, the radiation resistance R_R and the loss resistance R_L. The power associated with the radiation resistance is the power actually radiated by the antenna, while the power dissipated in the loss resistance is lost as heat in the antenna itself due to dielectric or conducting losses.

Both the real and imaginary parts of the impedance vary as a function of frequency. Ideally both the resistance and reactance exhibit symmetry about the resonant frequency and the reactance at resonance is equal to the average of sum of its maximum value (which is positive) and its minimum value (which is negative).

2.4.2 Voltage Standing Wave Ratio (VSWR)

In telecommunications, standing wave ratio (SWR) is the ratio of the amplitude of a partial standing wave at antinodes (maximum) to the amplitude at an adjacent node (minimum), in an electrical transmission line. The SWR is usually defined as a voltage ratio called the VSWR, for voltage standing wave ratio [10].

In a transmission line, the ratio of maximum to minimum voltage in a standing wave pattern is called the Voltage Standing Wave Ratio or VSWR. The voltage standing wave ratio is a measure of how well a load is impedance-matched to a source.

In order for the antenna to operate efficiently, maximum transfer of power must take place between the transmitter and the antenna shown in figure 2.3. Maximum power transfer can take place only when the impedance of the antenna (Z_{in}) is matched to that of the transmitter (Z_s).

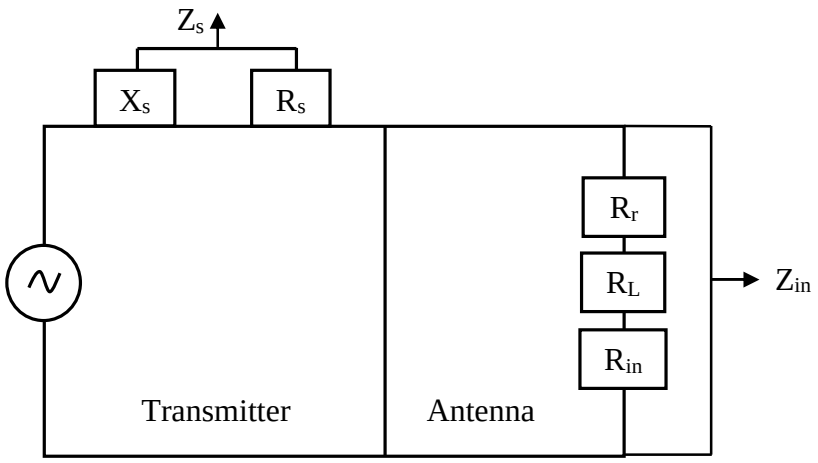

Figure 2.3: Equivalent Circuit of Transmitting Antenna.

According to the maximum power transfer theorem, maximum power can be transferred only if the impedance of the transmitter is a complex conjugate of the impedance of the antenna under consideration and vice-versa. Thus, the condition for matching is,

$$Z_{in} = Z_s^* \tag{2.2}$$

Where

$Z_{in} = R_{in} + jX_s$

$Z_s = R_s + jX_s$

If the condition for matching is not satisfied, then some of the power maybe reflected back and this leads to the creation of standing waves, which can be characterized by the parameter Voltage Standing Wave Ratio (VSWR). The VSWR is given as [10]

$$VSWR = \frac{1+|\Gamma|}{1-|\Gamma|} \tag{2.3}$$

Where

$$\Gamma = \frac{V_r}{V_i} = \frac{Z_{in} - Z_s}{Z_{in} + Z_s} \tag{2.4}$$

Where

Γ is called the reflection coefficient

V_r is the amplitude of the reflected wave

V_i is the amplitude of the incident wave

The VSWR is basically a measure of the impedance mismatch between the transmitter and the antenna. The minimum VSWR which corresponds to a perfect match is unity. A practical antenna design should have an input impedance of either 50 Ω or 75 Ω since most radio equipment is built for this impedance

2.4.3 Return Loss (RL)

The Return Loss (RL) is a parameter which indicates the amount of power that is lost to the load and does not return as a reflection. It is the ratio of the power reflected back from the line to the power transmitted into the line. As explained in the preceding section, waves are reflected leading to the formation of standing waves, when the transmitter and antenna impedance do not match. Hence the RL is a parameter similar to the VSWR to indicate how well the matching between the transmitter and antenna has taken place. The RL is expressed as a ratio in decibels (dB) [8].

$$RL = 10\log_{10}\frac{P_i}{P_r} \tag{2.5}$$

Where,

RL (dB) is the return loss in dB,

P_i is the incident power and

P_r is the reflected power.

Return loss is the negative of the magnitude of the reflection coefficient in dB. Since power is proportional to the square of the voltage, return loss is given by,

$$RL(dB) = -20\log_{10}|\Gamma| \tag{2.6}$$

For perfect matching between the transmitter and the antenna, $\Gamma = 0$ and $RL = \infty$ which means no power would be reflected back, whereas a $\Gamma = 1$ has a $RL = 0$ dB, which implies that all incident power is reflected. For practical applications, a VSWR of 2 is acceptable, since this corresponds to a RL of -9.54 dB.

2.4.4 Bandwidth

The bandwidth of an antenna is defined as the range of frequencies within which the performance of the antenna, with respect to some characteristic, conforms to a specified standard. The bandwidth can be considered to be the range of frequencies, on either side of a center frequency usually the resonance frequency for a dipole, where the antenna characteristics such as input impedance, radiation pattern, beam-width, polarization, gain, beam direction, radiation efficiency are within an acceptable value of those at the center frequency [8]. For broadband antennas, the bandwidth is usually expressed as the ratio of the upper-to-lower frequencies of acceptable operation. For narrowband antennas, the bandwidth is expressed as a percentage of the frequency difference (upper minus lower) over the center frequency of the bandwidth. Because the characteristics (input impedance, pattern, gain, and polarization, etc) of an antenna do not necessarily vary in the same manner or are even critically affected by the frequency, there is no unique characterization of the bandwidth. For intermediate length antennas, the bandwidth may be limited by either pattern or impedance variations, depending upon the particular application. For these antennas, a 2:1 bandwidth indicates a good design. For others, large bandwidths are needed. It is possible to increase the acceptable frequency range of a narrowband antenna if proper adjustments can be made on the critical dimensions of the antenna and/or on the coupling networks as the frequency is changed. According to these definitions bandwidth can be written in terms of equations as follows,

$$BW_{broadband} = \frac{f_h}{f_L} \tag{2.7}$$

$$BW_{broadband}(\%) = \left[\frac{f_H - f_L}{f_C}\right] 100\% \quad (2.8)$$

Where,

f_H = Upper frequency

f_L = Lower frequency

f_C = Center frequency

2.4.5 Directivity

The directivity of an antenna has been defined as the ratio of the radiation intensity in a given direction from the antenna to the radiation intensity average over all directions. In other words, the directivity of a non-isotropic source is equal to the ratio of its radiation intensity in a given direction, over that of an isotropic source. In mathematical form using, it can be written as [11],

$$\text{Directivity D} = \frac{\text{Maximum radiation intensity of the test antenna}}{\text{Average radiation intensity of the test antenna}}$$

$$D = \frac{U}{U_0} = \frac{2\pi U}{P_{rad}} \quad (2.9)$$

Sometimes, the direction of the directivity is not specified. In this case, the direction of the maximum radiation intensity is implied and the maximum directivity is given as [8],

$$D_{max} = \frac{U_{max}}{U_0} = \frac{2\pi U_{max}}{P_{rad}} \quad (2.10)$$

Where

D = Directivity of the test antenna (dimensionless)

D_{max} = Maximum directivity (dimensionless)

U = Radiation intensity of the test antenna (W/unit solid angle)

U_0 = Radiation intensity of an isotropic antenna (W/unit solid angle)

U_{max} = Maximum radiation intensity (W/unit solid angle)

P_{rad} = Total radiated power (W)

Generally D > 1, except in the case of an isotropic antenna for which D = 1. An antenna with directivity D >> 1 is a directive antenna.

Directivity is a dimensionless quantity, since it is the ratio of two radiation intensities. Generally directivity expressed in dB. The directivity of an antenna can be easily estimated from the

radiation pattern of the antenna. An antenna that has a narrow main lobe would have better directivity, then the one which has a broad main lobe, hence it is more directives.

2.4.6 Gain

The ratio of radiation intensity in a given direction to the maximum radiation intensity from a reference antenna in the same direction with the same input power is the gain of antenna. For microwave antennas, the reference antenna would be the isotropic antenna [11],

$$\text{Gain} = \frac{\text{Maximum radiation intensity from test antenna}}{\text{Radiaton intensity from isotropic antenna with same power input}}$$

$$\text{Gain} = 4\pi \frac{\text{Radiation intensity}}{\text{Total (accepted) input power}}$$

$$= 4\pi \frac{U(\theta,\varphi)}{P_{in}} (\text{dimensionless}) \qquad (2.11)$$

When the direction is not confirmed, the power gain is usually taken in the direction of maximum radiation. Than the directivity is how much an antenna concentrates energy in one direction in preference to radiation in other directions. Hence, if the antenna is 100% efficient, then the directivity would be equal to the antenna gain and the antenna would be an isotropic radiator. Since all antennas will radiate more in some direction that in others, therefore the gain is the amount of power that can be achieved in one direction at the expense of the power lost in the others. The gain is always related to the main lobe and is specified in the direction of maximum radiation unless indicated. According to the IEEE Standards, “gain does not include losses arising from impedance mismatches (reflection losses) and polarization mismatches [8].

2.4.7 Radiation Pattern

The radiation pattern is a graphical representation of radiation properties as a function of space co-ordinates. It shows the variation in actual field strength of electromagnetic field at all points which are at equal distance from the antenna. If the radiation from antenna is expressed in terms of field strength, the radiation pattern is called ‘Filed Strength Pattern’, and if in terms of power then ‘Power Pattern’ [11].

Most antennas show a pattern of ‘lobes’ or maxima of radiation. In a directive antenna, shown in figure 2.4, the largest lobe, in the desired direction of propagation, is called the ‘main lobe’. Back lobe is the minor lobe diametrically opposite to the main lobe.

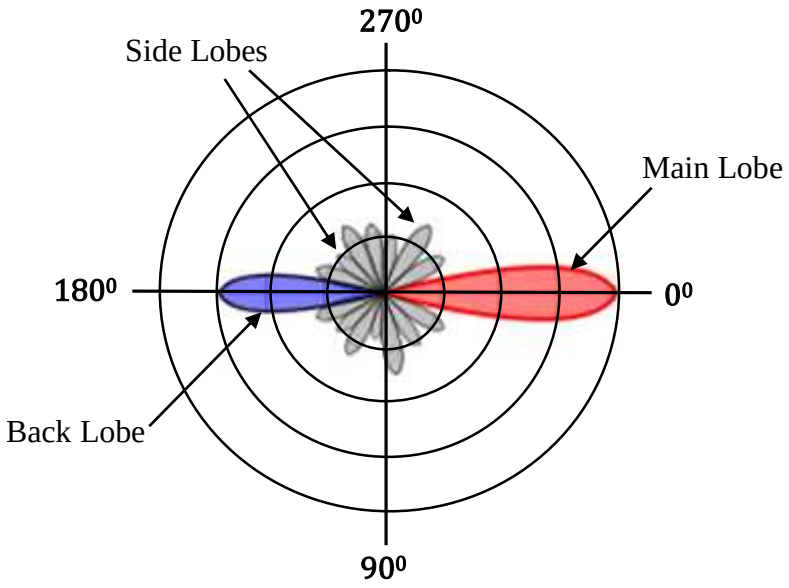

Figure 2.4: Radiation Pattern.

Side lobes are the minor lobes adjacent to the main lobe and are separated by various nulls. Side lobes are generally the largest among the minor lobes. In most wireless systems, minor lobes represent radiation in unwanted directions and are undesired. Hence a good antenna design should minimize the minor lobes.

Often the field and power patterns are normalized with respect to their maximum value, yielding normalized field and power patterns. Also, the power pattern is usually plotted on a logarithmic scale or more commonly in decibels (dB). This scale is usually desirable because a logarithmic scale can accentuate in more details those parts of the pattern that have very low values, refer to as minor lobes.

The radiation pattern of an antenna is a plot of the far-field radiation properties of an antenna as a function of the spatial co-ordinates which are specified by the elevation angle θ and the azimuth angle φ. More specifically it is a plot of the power radiated from an antenna per unit solid angle which is nothing but the radiation intensity. Consider the case of an isotropic antenna. An isotropic antenna is one which radiates equally in all directions.

If the total power radiated by the isotropic antenna is P, then the power is spread over a sphere of radius r, so that the power density S at this distance in any direction is given as,

$$S = \frac{P}{area} = \frac{P}{4\pi r^2} \tag{2.12}$$

Then the radiation intensity for this isotropic antenna U_i can be written as,

$$U_i = r^2 S = \frac{P}{4\pi} \tag{2.13}$$

An isotropic antenna is not possible to realize in practice and is useful only for comparison purposes. A more practical type is the directional antenna which radiates more power in some directions and less power in other directions. A special case of the directional antenna is the Omni-directional antenna whose radiation pattern may be constant in one plane (e.g. E-plane) and varies in an orthogonal plane (e.g. H-plane).

2.4.8 Efficiency

Efficiency is the ratio of power radiated to the total input power supplied to the antenna [11].

$$\text{Efficiency } \eta = \frac{\text{Power raidated}}{\text{Total input power}}$$

$$\eta = \frac{P_r}{P_r + P_l} \tag{2.14}$$

Or,

$$\eta = \frac{G_p}{G_d} = \frac{P_r}{P_r + P_l} \tag{2.15}$$

Where

P_r = Power radiated

P_l = Ohmic loses

G_p = Power gain or Gain

G_d = Directive gain

For the designer of microstrip antennas, the power carried by surface waves is an important parameter. This power has to be considered as a loss because it is trapped in the dielectric substrate. Moreover, unwanted radiation results when the surface wave encounters a discontinuity (e.g. the edge of the substrate). A parameter used to quantify this loss is the space

wave efficiency which relates the power radiated in space waves to the total radiated power (including surface waves). It is defined as follows

$$\eta = \frac{P_{sp}}{P_{sp} + P_{su}} \tag{2.16}$$

Where

P_{sp} = Power radiated in space waves

P_{su} = Power radiated in the surface wave.

If current flowing in the antenna is I, then form equation (2.14)

$$\eta = \frac{I^2 R_r}{I^2 (R_r + R_l)} \tag{2.17}$$

Or,

$$\eta\% = \frac{R_r}{R_r + R_l} \times 100 \tag{2.18}$$

Where,

R_r = Radiation resistance

R_l = Ohmic loss resistance of antenna conductor

$R_r + R_l$ = Total effective resistance

For better radiation characteristics from the antenna this loss resistances should be as small as possible. The loss resistances may consist of the following

- Ohmic loss in the antenna conductor.
- Dielectric loss.
- I^2R_g loss in antenna and ground system.
- Loss in earth connections.
- Leakage loss in insulation.

Thus antenna efficiency represents the fraction of total energy supplied to the antenna which is converted to electromagnetic waves [11].

2.4.9 Polarization

Polarization, also called wave polarization, is an expression of the orientation of the lines of electric flux in an electromagnetic field (EM field). Polarization can be constant; that is, existing in a particular orientation at all times, or it can rotate with each wave cycle.

Polarization is important in wireless communications systems. The physical orientation of a wireless antenna corresponds to the polarization of the radio waves received or transmitted by that antenna. Thus, a vertical antenna receives and emits vertically polarized waves, and a horizontal antenna receives or emits horizontally polarized waves.

The most common types of polarization include the linear (horizontal or vertical) and circular (right hand polarization or the left hand polarization).

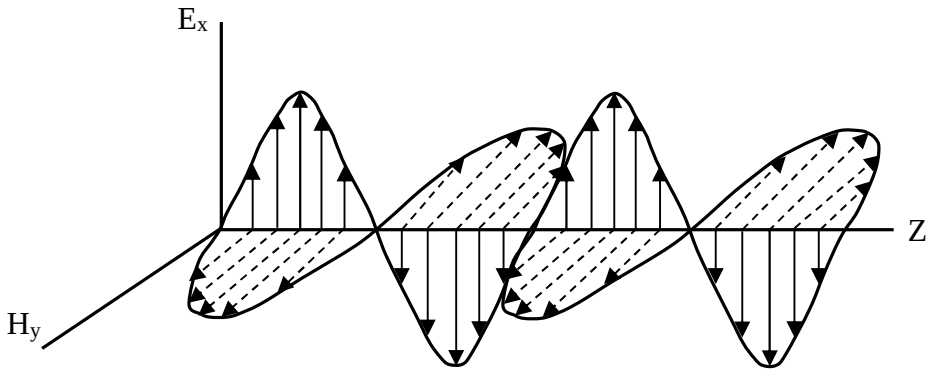

Figure 2.5: Linearly Polarized Wave.

If the path of the electric field vector is back and forth along a line, it is said to be linearly polarized. Figure 2.5 shows a linearly polarized wave. In a circularly polarized wave, the electric field vector remains constant in length but rotates around in a circular path. A left hand circular polarized wave is one in which the wave rotates counterclockwise whereas right hand circular polarized wave exhibits clockwise motion. Various polarization schemes are shown in figure 2.6.

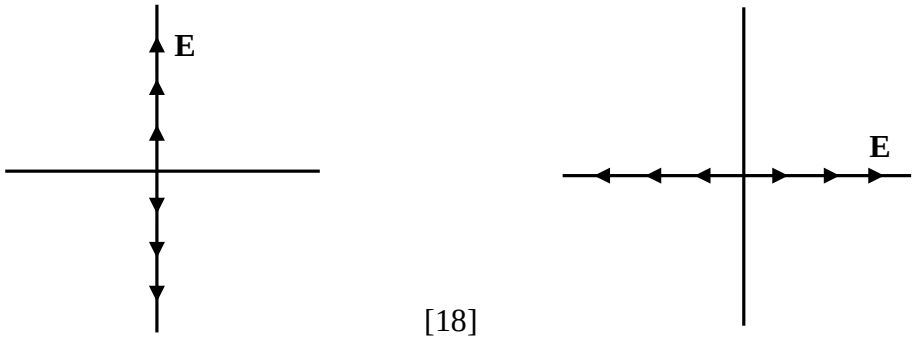

Vertical Linear Polarization

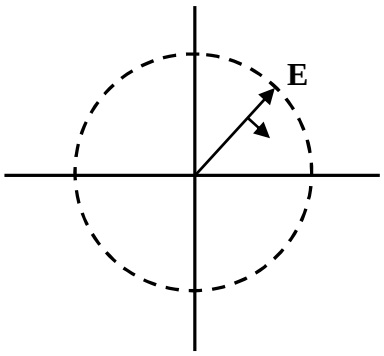

Horizontal Linear Polarization

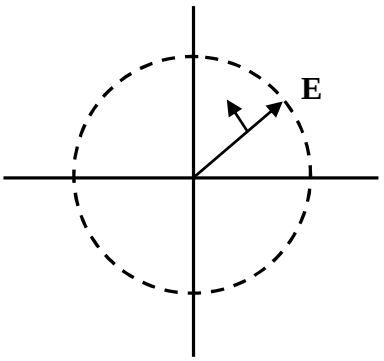

Right Hand Circular Polarization

Left Hand Circular Polarization

Figure 2.6: Various Polarization Schemes.

CHAPTER 3

Microstrip Patch Antenna

In this chapter, an introduction to the microstrip Patch Antenna has followed by its advantages and disadvantages. Next, theoretical structure of proposed patch antenna and some feed modeling techniques has been discussed. Also represent an introduction to the split ring resonator with its advantages and disadvantages. Finally, a detailed explanation of microstrip patch antenna analysis has been explained.

3.1 Introduction

Communication has expanded much rapidly in the past couple of decades, and the ever expanding need of communication bandwidth defines new communication protocols which in turn expect better technology to fill in the gap. Microstrip patch antenna has attracted lots of interest in the field of mobile communication due to its important characteristics along with easy to achieve multi frequency operation and relatively large area consumption.

The exploding growth of wireless communication systems leads to an increasing demand for the multilayered laminates broadband compact low-cost microstrip antennas. The low profile multilayer microstrip antennas with a broadband and constant gain for wireless communication systems are now of great interest owing to the increase in the data rate [12].

To improve the performance of microstrip antennas, many techniques have been employed. The standard processing steps found in a boundary fit quite well the need to fabricate a standard patch antenna. The main challenge is the material to be used as substrate. Parameters like substrate thickness, dielectric permittivity, dielectric losses, metal conductivity and thickness, should be evaluated to understand its influence on overall antenna performance. Most of works is going the research in the matter of making light and low cost device.

3.2 Microstrip Patch Antenna

A patch antenna (also known as a rectangular microstrip antenna) is a type of radio antenna with a low profile, which can be mounted on a flat surface. It consists of a flat rectangular sheet or "patch" of metal, mounted over a larger sheet of metal called a ground plane.

A microstrip patch antenna consists of a radiating patch on one side of a dielectric substrate which has a ground plane on the other side. The patch is generally made of conducting material, can take any possible shape. The radiating patch and the feed lines are usually photo etched on the dielectric substrate which is shown in the figure 3.1.

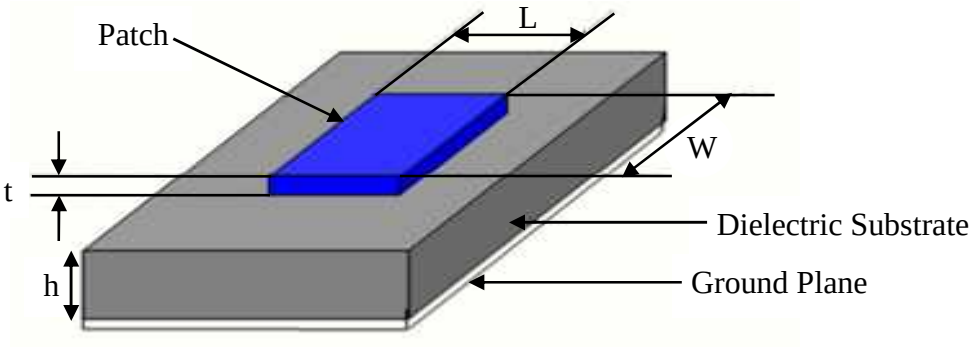

Figure 3.1: Structure of a Microstrip Patch Antenna.

In order to simplify analysis and performance prediction, the patch is generally square, rectangular, circular, triangular and elliptical or some other comm on shape as shown in figure 3.2 [8].

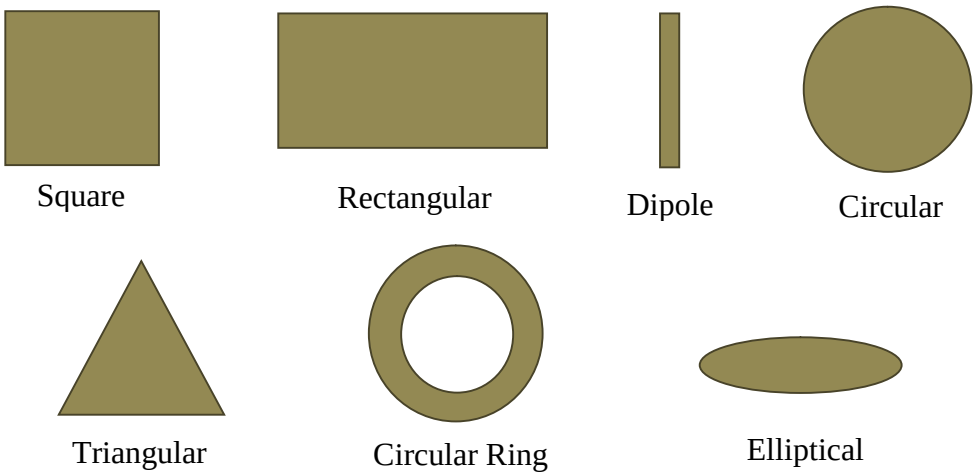

Figure 3.2: Common Shapes of Microstrip Patch Elements.

Microstrip patch antennas radiate primarily because of the fringing fields between the patch edge and the ground plane. For good antenna performance, a thick dielectric substrate having a low dielectric constant is desirable since this provides better efficiency, larger bandwidth and better radiation.

3.3 Advantages and Disadvantages of Microstrip Patch Antenna

Microstrip patch antennas are increasing in popularity for use in wireless applications due to their low-profile structure. Therefore they are extremely compatible for embedded antennas in handheld wireless devices such as cellular phones, pagers etc. The telemetry and communication antennas on missiles need to be thin and conformal and are often Microstrip patch antennas. Another area where they have been used successfully is in Satellite communication. Some of their principal advantages are given below

- Light weight and low volume.
- Low profile planar configuration which can be easily made conformal to host surface.
- Low fabrication cost, hence can be manufactured in large quantities.
- Supports both, linear as well as circular polarization.
- Can be easily integrated with microwave integrated circuits (MICs).
- Capable of dual and triple frequency operations.
- Mechanically robust when mounted on rigid surfaces.

Microstrip patch antennas suffer from a number of disadvantages as compared to conventional antennas. Some of their major disadvantages are given below

- Narrow bandwidth
- Low efficiency
- Low Gain
- Extraneous radiation from feeds and junctions
- Poor end fire radiator except tapered slot antennas
- Low power handling capacity.
- Surface wave excitation

3.4 Basic characteristics

Microstrip antennas, as shown in figure 3.3(a) consist of a very thin ($t << \lambda_0$ where λ_0 is the free-space wavelength) metallic strip (patch) placed a small fraction of a wave-length ($h << \lambda_0$ usually $0.003\lambda_0 \leq h \leq 0.05\ \lambda_0$) above a ground plane. For a rectangular patch, the length L of the element is usually $\lambda_0/3 < L < \lambda_0/2$. The strip (patch) and the ground plane are separated by a dielectric sheet (referred to as the substrate), as shown in above figure 3.1 [8].

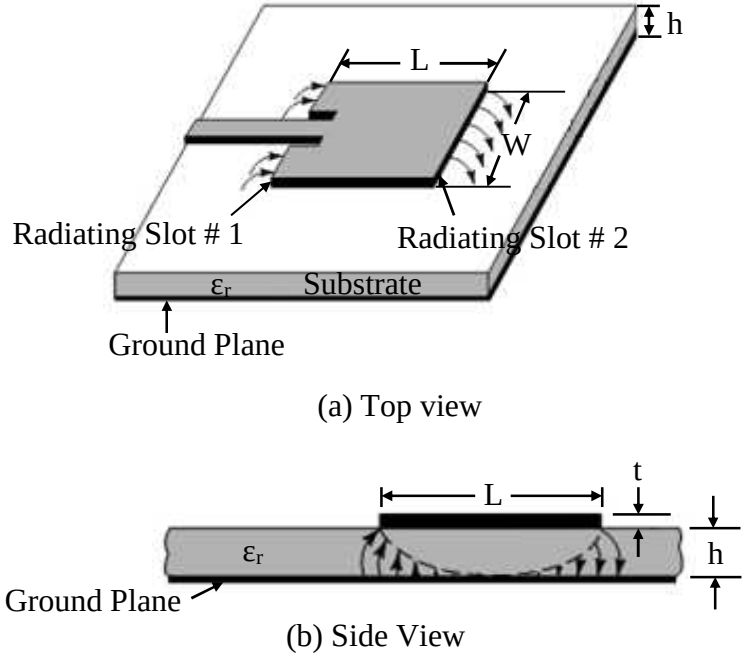

Figure 3.3: Microstrip Antenna (Top View and Side View).

There are numerous substrates that can be used for the design of microstrip antennas, and their dielectric constants (ε_r) are usually in the range of $2.2 \leq \varepsilon_r \leq 12$. The ones that are most desirable for good antenna performance are thick substrates whose dielectric constant is in the lower end of the range because they provide better efficiency, larger bandwidth, loosely bound fields for radiation into space, but at the expense of larger element size. Thin substrates with higher dielectric constants are desirable for microwave circuitry because they require tightly bound fields to minimize undesired radiation and coupling, and lead to smaller element sizes.

3.5 Feeding Methods

There are various feeding methods of microstrip antenna. These methods can be classified into two categories- contacting and non-contacting. In the contacting method, the RF power is fed directly to the radiating patch using a connecting element such as a microstrip line. In the non-contacting scheme, electromagnetic field coupling is done to transfer power between the microstrip line and the radiating patch. The four most popular feed techniques used are [8],

- The microstrip line,
- Coaxial probe (both contacting schemes),
- Aperture coupling and
- Proximity coupling (both non-contacting schemes).

3.5.1 Microstrip Line Feed

In this type of feed technique, a conducting strip is connected directly to the edge of the microstrip patch as shown in figure 3.4. The conducting strip is smaller in width as compared to the patch and this kind of feed arrangement has the advantage that the feed can be etched on the same substrate to provide a planar structure [8].

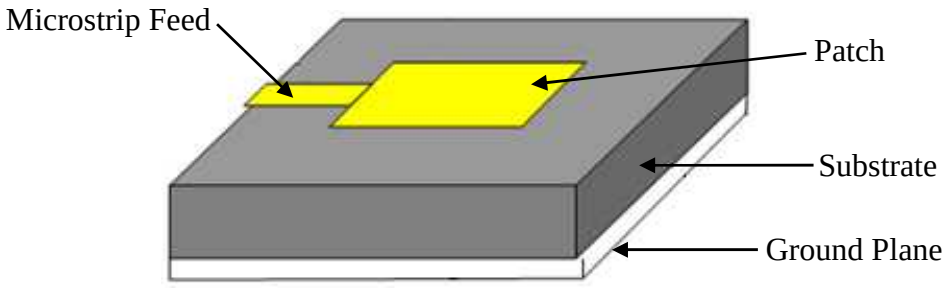

Figure 3.4: Microstrip Line Feed.

The purpose of the inset cut in the patch is to match the impedance of the feed line to the patch without the need for any additional matching element. This is achieved by properly controlling the inset position. However as the thickness of the dielectric substrate being used, increases, surface waves and spurious feed radiation also increases, which hampers the bandwidth of the antenna. The feed radiation also leads to undesired cross polarized radiation.

3.5.2 Coaxial Probe Feed

The Coaxial feed or probe feed is a very common technique used for feeding microstrip patch antennas. As seen from figure 3.5, the inner conductor of the coaxial connector extends through the dielectric and is soldered to the radiating patch, while the outer conductor is connected to the ground plane. The main advantage of this type of feeding scheme is that the feed can be placed at any desired location inside the patch in order to match with its input impedance. This feed method is easy to fabricate and has low spurious radiation [8].

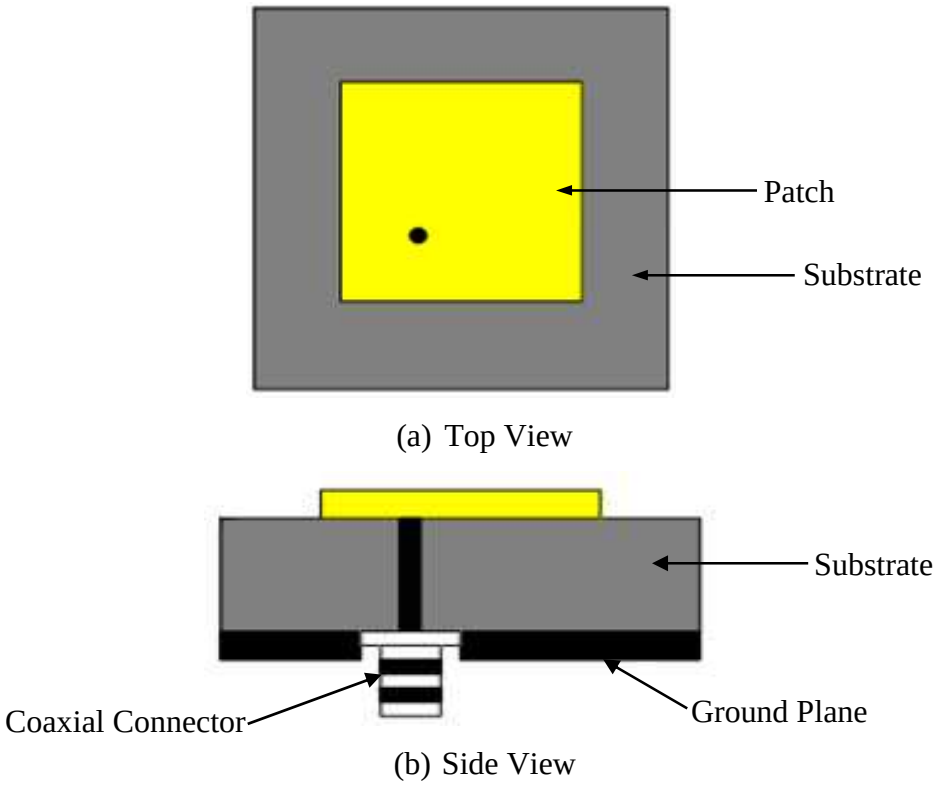

Figure 3.5: Probe Fed Rectangular Microstrip Patch Antenna

However, its major disadvantage is that it provides narrow bandwidth and is difficult to model since a hole has to be drilled in the substrate and the connector protrudes outside the ground plane, thus not making it completely planar for thick substrates ($h > 0.02\lambda_0$). Also, for thicker substrates, the increased probe length makes the input impedance more inductive, leading to matching problems.

3.5.3 Aperture Coupled Feed

In this type of feed technique, the radiating patch and the microstrip feed line are separated by the ground plane as shown in figure 3.6. Coupling between the patch and the feed line is made through a slot or an aperture in the ground plane.

The coupling aperture is usually centered under the patch, leading to lower cross-polarization due to symmetry of the configuration. The amount of coupling from the feed line to the patch is determined by the shape, size and location of the aperture. Since the ground plane separates the patch and the feed line, spurious radiation is minimized. Generally, a high dielectric material is used for the bottom substrate and a thick, low dielectric constant material is used for the top substrate to optimize radiation from the patch [8].

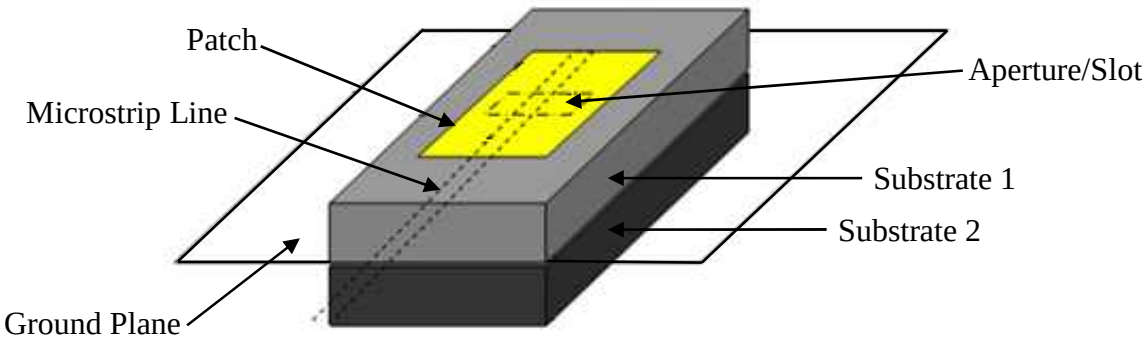

Figure 3.6: Aperture-Coupled Feed.

The major disadvantage of this feed technique is that, it is difficult to fabricate due to multiple layers, which also increases the antenna thickness. This feeding scheme also provides narrow bandwidth.

3.5.4 Proximity Coupled Feed

This type of feed technique is also called as the electromagnetic coupling scheme. As shown in figure 3.7, two dielectric substrates are used such that the feed line is between the two substrates and the radiating patch is on top of the upper substrate. The main advantage of this feed technique is that it eliminates spurious feed radiation and provides very high bandwidth, due to overall increase in the thickness of the microstrip patch antenna. This scheme also provides

choices between two different dielectric media, one for the patch and one for the feed line to optimize the individual performances [8].

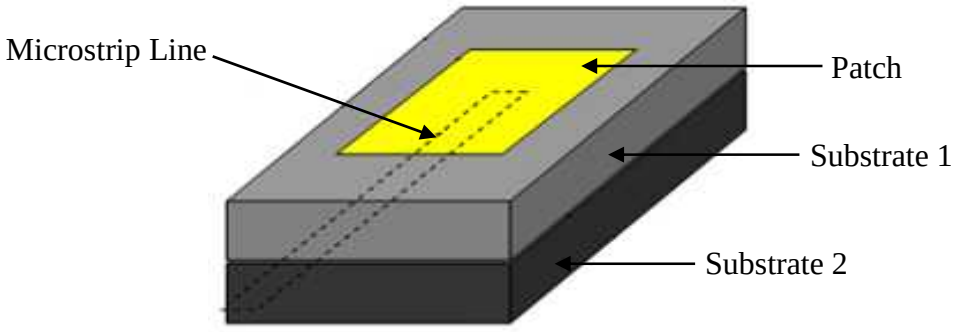

Figure 3.7: Proximity-Coupled Feed.

Matching can be achieved by controlling the length of the feed line and the width-to-line ratio of the patch. The major disadvantage of this feed scheme is that it is difficult to fabricate because of the two dielectric layers which need proper alignment. Also, there is an increase in the overall thickness of the antenna. Table 3.1 summarizes the characteristics of the different feed techniques.

Table 3.1: Comparison between Different Feeding Techniques

Characteristics	Microstrip Line Feed	Coaxial Feed	Aperture coupled Feed	Proximity coupled Feed
Spurious feed radiation	More	More	Less	Minimum
Reliability	Better	Better due to soldering	Good	Good
Ease of fabrication	Easy	Soldering and drilling needed	Alignment required	Alignment required
Impedance Matching	Easy	Easy	Easy	Easy
Bandwidth(achieved with impedance matching)	2-5%	2-5%	2-5%	13%

3.6 Theoretical Structure Analysis Method

The most popular models for the analysis of microstrip patch antennas are the transmission line model, cavity model, and full wave model. The transmission line model is the simplest of all and it gives good physical insight but it is less accurate. The cavity model is more accurate and gives

good physical insight but is complex in nature. The full wave models are extremely accurate, versatile and can treat single elements, finite and infinite arrays, stacked elements, arbitrary shaped elements and coupling. These give less insight as compared to the two models mentioned above and are far more complex in nature [13].

The rectangular patch is the most widely used configuration. It is very easy to analyze using both the transmission-line and cavity models, which are most accurate for thin substrates. We begin with the transmission-line model because it is easier to illustrate.

3.6.1 Transmission Line Model

This model represents the microstrip antenna by two slots of width W and height h, separated by a transmission line of length L. The microstrip is essentially a non-homogeneous line of two dielectrics, typically the substrate and air [8].

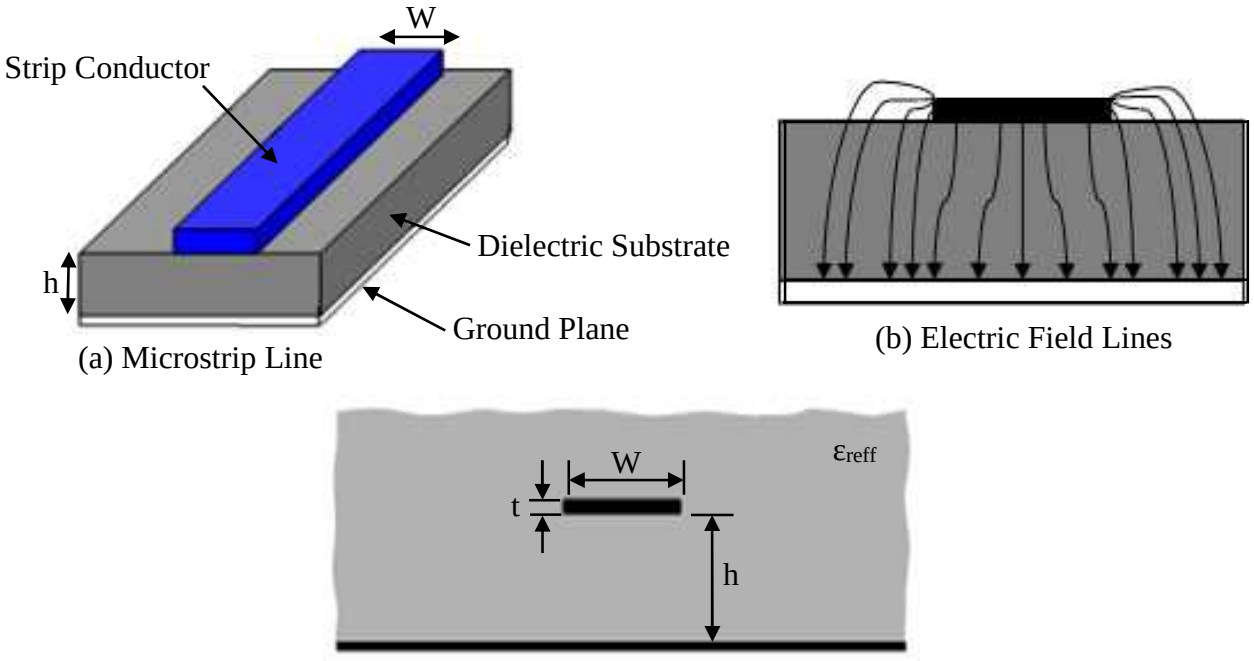

Figure 3.8: Microstrip Line, Its Electric Field Lines, and Effective Dielectric Constant Geometry.

3.6.2 Fringing Effects

Because the dimensions of the patch are finite along the length and width, the fields at the edges of the patch undergo fringing. This is illustrated along the length in figures 3.8(a and b) for the two radiating slots of the microstrip antenna. The same applies along the width. The amount of fringing is a function of the dimensions of the patch and the height of the substrate. For the principal E-plane (xy-plane) fringing is a function of the ratio of the length of the patch L to the height h of the substrate (L/h) and the dielectric constant ε_r of the substrate. Since for microstrip antennas L/h >> 1, fringing is reduced; however, it must be taken into account because it influences the resonant frequency of the antenna [8]. The same applies for the width.

Hence, as seen from Figure 3.8(b), most of the electric field lines reside in the substrate and parts of some lines in air. As a result, this transmission line cannot support pure transverse-electric-magnetic (TEM) mode of transmission, since the phase velocities would be different in the air and the substrate. Instead, the dominant mode of propagation would be the quasi-TEM mode [13]. Hence, an effective dielectric constant (ε_{reff}) must be obtained in order to account for the fringing and the wave propagation in the line. The value of ε_{reff} is slightly less than ε_r because the fringing fields around the periphery of the patch are not confined in the dielectric substrate but are also spread in the air as shown in Figure 14.5(b) above. The expression for ε_{reff} is given by,

$$\varepsilon_{reff} = \frac{\varepsilon_r + 1}{2} + \frac{\varepsilon_r - 1}{2}\left[1 + 12\frac{h}{W}\right]^{-1/2} \quad (3.1)$$

Where

ε_{reff} = Effective dielectric constant

ε_r = Dielectric constant of substrate

h = Height of dielectric substrate

W = Width of the patch

3.6.3 Effective Length, Resonant Frequency and Width

Consider figure 3.9 below, which shows a rectangular microstrip patch antenna of length L, width W resting on a substrate of height h. The co-ordinate axis is selected such that the length is along the x direction, width is along the y direction and the height is along the z direction.

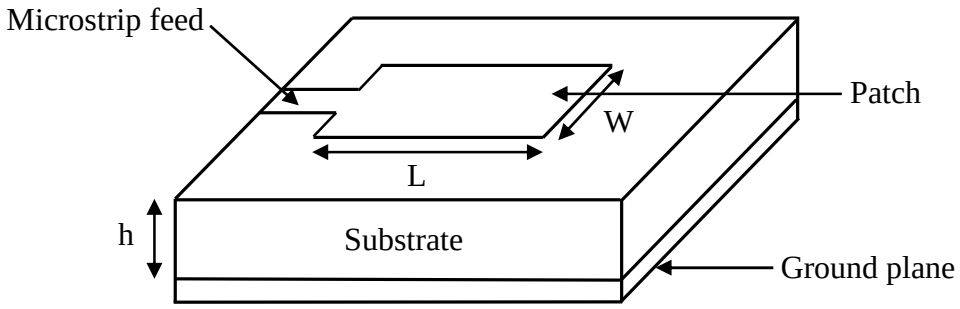

Figure 3.9: Microstrip Patch Antenna.

In order to operate in the fundamental TM_{10} mode, the length of the patch must be slightly less than λ/2 where λ is the wavelength in the dielectric medium and is equal to $\lambda_0/\sqrt{\varepsilon_{reff}}$ where λ_0 is the free space wavelength [14]. The TM_{10} mode implies that the field varies one λ/2 cycle along the length, and there is no variation along the width of the patch. In the figure 3.10 shown below, the microstrip patch antenna is represented by two slots, separated by a transmission line of length L and open circuited at both the ends. Along the width of the patch, the voltage is maximum and current is minimum due to the open ends. The fields at the edges can be resolved into normal and tangential components with respect to the ground plane.

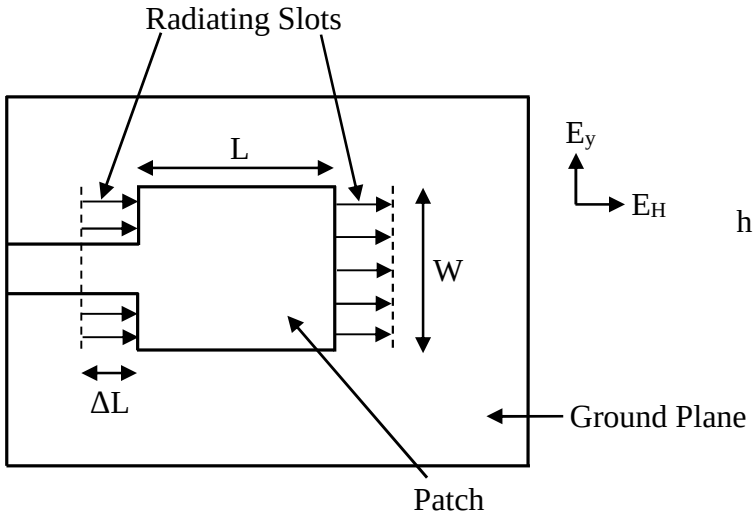

Figure 3.10: Top View of Antenna.

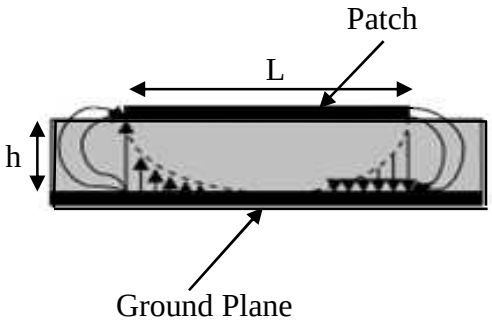

Figure 3.11: Side View of Antenna.

It is seen from figure 3.11 that the normal components of the electric field at the two edges along the width are in opposite directions and thus out of phase since the patch is λ/2 long and hence they cancel each other in the broadside direction. The tangential components (seen in Figure 3.11), which are in phase, means that the resulting fields combine to give maximum radiated field normal to the surface of the structure. Hence the edges along the width can be represented as two radiating slots, which are λ/2 apart and excited in phase and radiating in the half space above the ground plane. The fringing fields along the width can be modeled as radiating slots and electrically the patch of the microstrip antenna looks greater than its physical dimensions. The dimensions of the patch along its length have now been extended on each end by a distance ΔL, which is a function of the effective dielectric constant ε_{reff} and the width-to-height ratio (W/h), given as [8]

$$\Delta L = 0.12h\frac{(\varepsilon_{reff}+0.3)\left(\frac{W}{h}+0.26\right)}{(\varepsilon_{reff}-0.258)\left(\frac{W}{h}+0.8\right)} \tag{3.2}$$

Hence the length of the patch has been extended by ΔL on each side, the effective length of the patch L_{eff} which is given by,

$$L_{eff} = L + 2\Delta L \tag{3.3}$$

For a given resonance frequency f_0, the effective length is given by [8]

$$L_{eff} = \frac{c}{2f_0\sqrt{\varepsilon_{reff}}} \tag{3.4}$$

Where, c is the speed of light in the free space.

For a rectangular microstrip patch antenna, the resonance frequency for any TM_{mn} mode is given by,

$$f_0 = \frac{c}{2\sqrt{\varepsilon_{reff}}}\left[\left(\frac{m}{L}\right)^2+\left(\frac{n}{W}\right)^2\right]^{\frac{1}{2}} \tag{3.5}$$

Where, m and n are modes along L and W respectively.

For efficient radiation, the width W is given

$$W = \frac{c}{2f_0\sqrt{\frac{\varepsilon_r+1}{2}}} \tag{3.6}$$

The length and width of ground plane L_g and W_g are given as [8],

$$L_g = 6h + L \tag{3.7}$$

$$W_g = 6h + W \tag{3.8}$$

3.7 An Overview on Resonator

This is a device that oscillates naturally with greater amplitude at certain frequencies than at other frequencies. An LC circuit can be idealized as a resonant circuit; it consists of an inductor and a capacitor.

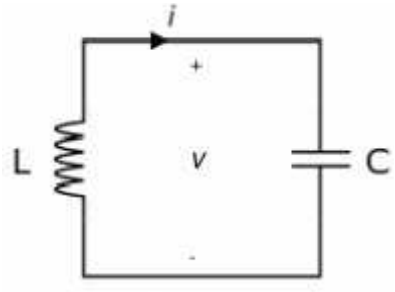

Figure 3.12: LC Circuit.

When the inductor and the capacitor are connected together, the resultant circuit can function as an electrical resonator. LC circuits have the capability of producing signals at a certain frequency and can also pick out a signal from a more complex signal at certain frequency. They form the prime components of numerous electronic devices, specifically radio equipment. They find good uses in filters, oscillators, tuners, and frequency mixers.

3.7.1 Resonance

Resonance occurs when capacitive reactance equals inductive reactance in magnitude and the frequency at which these two reactances hold for the specific circuit is termed the resonant frequency of that circuit.LC circuit has a resonant frequency which is written as

$$f_0 = \frac{1}{2\pi\sqrt{LC}}$$

There can be series and parallel resonant LC circuit for the series resonant circuit as the inductance rises and the capacitance decreases, the narrower the filter bandwidth becomes when

the LC circuit is used as a filter the opposite is true for a parallel resonant circuit. Figure 3.13 shows a series and parallel LC resonant circuits.

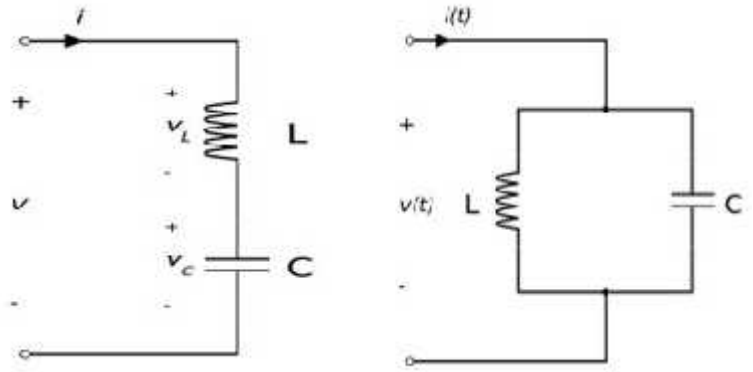

Figure 3.13: A Series and Parallel LC Resonant Circuits.

3.7.2 Uses of Resonator

- To generate waves of specific frequencies.
- To select specific frequencies from a signal.
- Used in oscillators and transformers to create microwave signals.
- Used as filters to separate a signal at a given frequency from others.
- Used in radar equipment.
- Used in microwave relay stations.
- Used in satellite communication.
- Used in microwave oven.
- Used in particle accelerators.

3.7.3 Types of resonators

Many types of resonators exist; they form essential parts of musical instruments, our voices, clocks and numerous electronics and communication circuits. They are present throughout natural phenomena ranging from atomic transitions, atoms, atomic nuclei to massive resonating stars and suns. Broadly, resonators are acoustic such as flutes and organ pipes, mechanical

such as bells and turning forks, atomic such as electrons found in atoms, and electronic such as LC circuits. The resonator in this project falls under the electronic type.

3.7.4 The Split Ring Resonator

The split ring resonators (SRR) often consist of two metallic rings, circular or square, carved or etched on dielectric substrates and they always have gaps on opposite sides. They have been employed for making left handed media with negative refractive index.

The splits in the rings make them support resonant wavelengths a lot larger than the diameters of the rings; a thing that is not obtainable in closed rings. Large values of capacitance are produced in the resonators due to the small gaps between the rings; the capacitance is inversely proportional to the resonant frequency of the ring. The resonant wavelength far outweighs the dimensions of the structure and this brings about high quality factor and low radiative losses [15-17].

The geometric parameters of the ring resonator and the resonant frequency are dependent on each other [18] and the structure has the capability of exhibiting resonance at frequencies much larger than its size [19]

3.7.5 Advantages and Disadvantage of Split Ring Resonator

Advantages

- Artificially produced structure
- Creates strong magnetic coupling
- To generate waves of specific frequencies.
- It provides a strong support to create microwave signals.
- It can filter to separate a signal at a given frequency from others.

Disadvantages

- It possesses a fundamental disadvantage of large size.
- It can be designed to inductively narrow frequency band.
- Construction of a rigid 2-D structure is too complex.

CHAPTER 4

Design & Methodology

In this chapter the procedure for designing a rectangular microstrip patch antenna with complementary triangular split ring resonator is explained. It has concentrated on the analysis of DETCSRR structure on patch antenna design, various distances between two ETCSRR structures, different size of DETCSRR structures, various orientations of resonant cut structures and corresponding key performance analysis results (resonant frequency, return loss, gain, and impedance bandwidth) have been demonstrated**.** At last the decision is made with respect to performance of our novel proposed cellular antenna.

4.1 Roger RT/Duroid Based Antenna

4.1.1 Design Calculation

The three essential parameters for the design of a rectangular microstrip patch antenna are given below,

- **Dielectric Constant of the Substrate (ε_r):** The dielectric material selected for our design is Roger RT/Duroid which has a dielectric constant of 2.2. A substrate with a moderate dielectric constant is selected since it reduces the dimension of our proposed antenna and for better performance.
- **Frequency of Operation (f_0):** The resonant frequency of the antenna must be selected appropriately. The Wireless Local Area Network (WLAN) or Wi-Fi uses the IEEE 802.11 which frequency range from 2400-2500 MHz that's why our proposed antenna must be able to operate in this frequency range. The frequency of operation for the patch antenna we are trying to design has been selected as 2.44 GHz.
- **Height of Dielectric Substrate (h):** Microstrip Patch antenna has been designed in order to rule out the conventional antenna as the patch antennas are used in most of the compact

devices**.** For the microstrip patch antenna to be used in cellular phones, it is essential that the antenna is not bulky [20]. Substrate thickness should be chosen as large as possible to maximize bandwidth and efficiency, but not so large as to risk surface-wave excitation. For maximum operating frequency fu the substrate thickness (h) should satisfy: [7]

$$h \leq \frac{0.3\,C}{2Bf_0\sqrt{\varepsilon_r}}$$

where, gr is the relative dielectric constant obtained using resonant line method and c is the light speed. Hence, the height of the dielectric substrate is 1.6mm.

Table 4.1: Essential Parameters for Roger RT/Duroid Based Design

$\varepsilon_r = 2.2$	$f_0 = 2.44$ GHz	h = 1.6 cm

4.1.2 Design Procedure

The transmission line model, described in the previous chapter will be used to design the antenna.

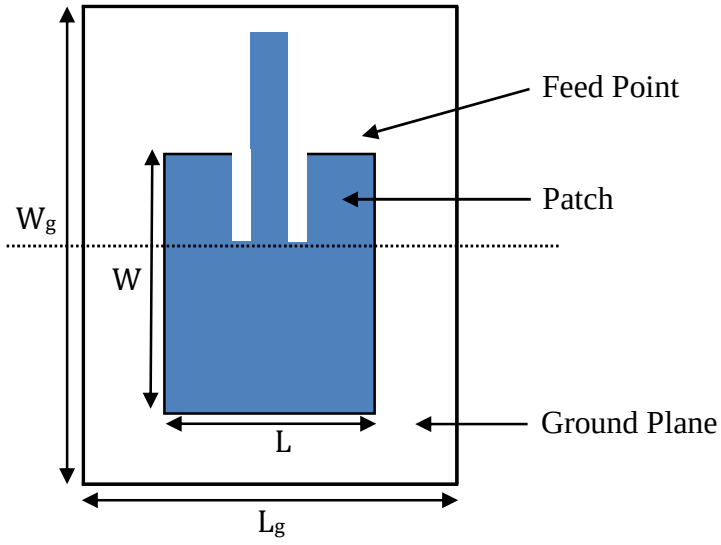

Figure 4.1 Top View of Microstrip Patch Antenna

Step 1: Calculation of the Width (W)

The width of the Microstrip patch antenna is given by the following formula

$$W = \frac{c}{2f_0\sqrt{\frac{\varepsilon_r + 1}{2}}} \tag{4.1}$$

Substituting, $c = 3\times10^8$ m/s, $\varepsilon_r = 2.2$ and $f_0 = 2.44$GHz, we get the value of width

$$\mathbf{W = 4.860\times 10^{-05}m = 48.60mm}$$

Step 2: Calculation of Effective Dielectric Constant (ε_{reff})

From the following equation we get the value of effective dielectric constant

$$\varepsilon_{reff} = \frac{\varepsilon_r + 1}{2} + \frac{\varepsilon_r - 1}{2}\left[1 + 12\frac{h}{W}\right]^{-1/2} \tag{4.2}$$

ε_{reff} = Effective dielectric constant

ε_r = Dielectric constant of substrate

h = Height of dielectric substrate

W = Width of the patch

Substituting, $\varepsilon_r = 2.2$, $W = 48.60$mm and $h = 1.6$ mm, we get

$$\varepsilon_{reff} = \mathbf{2.107}$$

Step 3: Calculation of the Effective Length (L_{eff})

Equation (3.4) gives the effective length as,

$$L_{eff} = \frac{c}{2f_0\sqrt{\varepsilon_{reff}}} \tag{4.3}$$

Substituting, $c = 3\times10^8$ m/s, $\varepsilon_{reff} = 2.107$ and $f_0 = 2.44$ GHz, we get

$$\mathbf{L_{eff} = 42.23mm}$$

Step 4: Calculation of the Length Extension (ΔL)

Equation (3.2) gives the effective length extension as

$$\Delta L = 0.12h\frac{(\varepsilon_{reff} + 0.3)\left(\frac{W}{h} + 0.26\right)}{(\varepsilon_{reff} - 0.258)\left(\frac{W}{h} + 0.8\right)} \tag{4.4}$$

Substituting, $\varepsilon_{reff} = 2.107$, $W = 48.60$mm and $h = 1.6$ mm, we get

$$\Delta L = 0.24mm$$

Step 5: Calculation of Actual Length of Patch (L)

The actual length is obtained by

$$L = L_{eff} - 2\Delta \tag{4.5}$$

Substituting $L_{eff} = 42.23mm$ and $\Delta L = 0.24mm$ we get,

$$L = 41.73mm$$

Step 6: Calculation of the Ground Plane Dimensions (L_g & W_g)

The transmission line model is applicable to infinite ground planes only. However, for practical considerations, it is essential to have a finite ground plane [21]. It has been shown by many engineers that similar results for finite and infinite ground plane can be obtained if the size of the ground plane is greater than the patch dimensions by approximately six times the substrate thickness all around the periphery. Hence, for this design, the ground plane dimensions would be given from equation (3.7) and (3.8) as

$$L_g = 6h + L = 51.33mm$$

$$W_g = 6h + W = 58.2mm$$

Step 7: Design of Triangular Split Ring Resonator

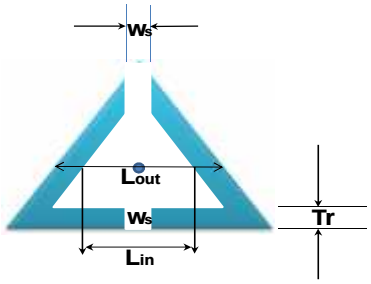

Figure 4.2: Top view of ETCSRR Structure

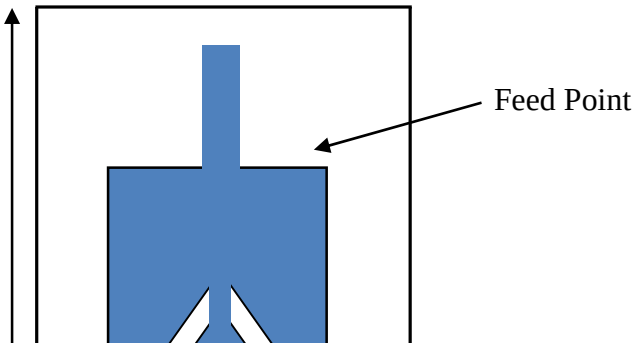

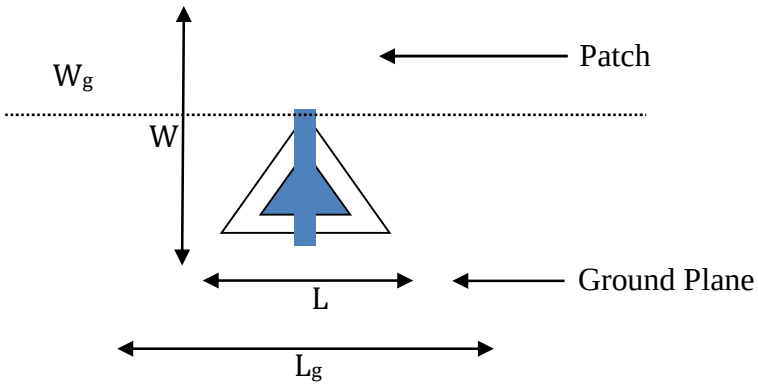

Figure 4.3 Top View of Microstrip Patch Antenna with ETCSRR.

Figure 4.2 shows the geometric view of the single unit of complementary triangular cut split ring resonator. The outer and inner length of the ETCSRR structure is L_{out}= 4.25mm and L_{in}= 3.25mm respectively. The dimension of the resonator gap W_s =0.98mm and the thickness of the triangle T_r=1mm.

Table 4.2: Various Dimensions of ETCSRR Structure

Part	Symbol	Dimension (mm)
Resonator outer width	L_{out}	4.25
Resonator inner width	L_{in}	3.25
Thickness of TSRR	Tr	1.00
Resonator gap	W_s	0.98

4.2 Radiation Intensity

Radiation intensity in a given direction is defined as “the power radiated from an antenna per unit solid angle.” The radiation intensity is a far-field parameter, and it can be obtained by simply multiplying the radiation density by the square of the distance. In mathematical form it is expressed as

$$U = r^2 W_{rad} \tag{4.6}$$

Where

U = radiation intensity (W/unit solid angle)

W_{rad} = radiation density (W/m2)

The radiation intensity is also related to the far-zone electric field of an antenna, referring to Figure 2.4, by

$$U(\theta,\varphi)=\frac{r^2}{2\eta}|E(r,\theta,\varphi)|^2 \approx \frac{r^2}{2\eta}\left[|E(r,\theta,\varphi)|^2+|E(r,\theta,\varphi)|^2\right] \approx \frac{1}{2\eta}\left[|E(\theta,\varphi)|^2+|E(\theta,\varphi)|^2\right] \quad (4.7)$$

Where

$E(r,\theta,\varphi)$ = Far-zone electric-field intensity of the antenna = $E(\theta,\varphi)\frac{e^{-jkr}}{r}$

E_θ, E_φ = Far-zone electric-field components of the antenna

η = Intrinsic impedance of the medium

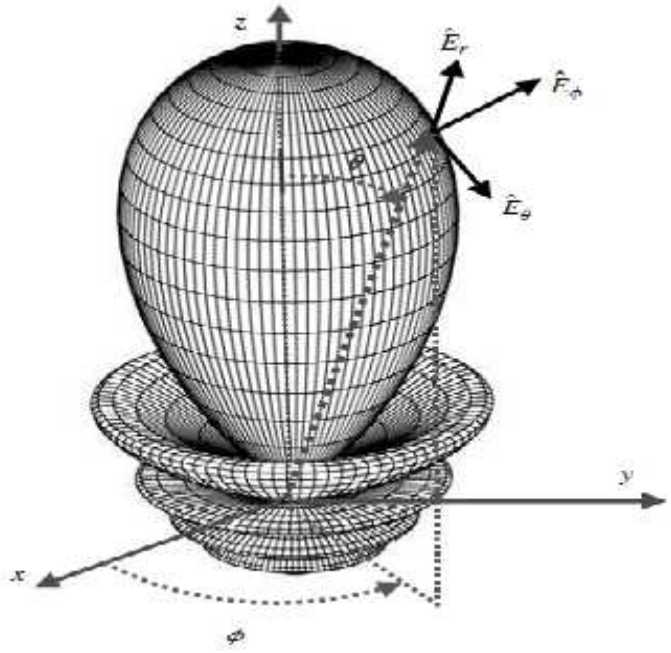

Figure 4.4 Normalized three-dimensional amplitude field pattern (in linear scale) of a10-ele ment linear array antenna with a uniform spacing of d = 0.25λ and progressive phase shift β =−0.6π between the elements.

The radial electric-field component (E_r) is assumed, if present, to be small in the far zone. Thus the power pattern is also a measure of the radiation intensity. The total power is obtained by integrating the radiation intensity, as given by (4.6), over the entire solid angle of 4π. Thus

$$P_{rad}=\oiint \Omega\, d\Omega=\int_0^{2\pi}\int_0^{\pi} U\sin\theta\, d\theta\, d\varphi \quad (4.8)$$

Where $d\Omega$ = element of solid angle $= \sin\theta d\theta d\varphi$

For anisotropic source U will be independent of the angles θ and φ, as was the case for W_{rad}. Thus (2-13) can be written as

$$P_{rad} = \oint\oint U_0 \, d\Omega = U_0 \oint\oint d\Omega = 4\pi U_0 \tag{4.9}$$

or the radiation intensity of an isotropic source as

$$U_0 = \frac{P_{rad}}{4\pi} \tag{4.10}$$

4.3 Directivity

Directivity of an antenna defined as "the ratio of the radiation intensity in a given direction from the antenna to the radiation intensity averaged over all directions. The average radiation intensity is equal to the total power radiated by the antenna divided by 4π. If the direction is not specified, the direction of maximum radiation intensity is implied." Stated more simply, the directivity of a nonisotropic source is equal to the ratio of its radiation intensity in a given direction over that of an isotropic source. In mathematical form, using (4.10), it can be written as

$$D = \frac{U}{U_0} = \frac{4\pi U}{P_{rad}} \tag{4.11}$$

If the direction is not specified, it implies the direction of maximum radiation intensity (maximum directivity) expressed as

$$D_{max} = D_0 = \frac{U|_{max}}{U_0} = \frac{U_{max}}{U_0} = \frac{4\pi U_{max}}{P_{rad}} \tag{4.12}$$

D = directivity (dimensionless)

D_0 = maximum directivity (dimensionless)

U = radiation intensity (W/unit solid angle)

U_{max} = maximum radiation intensity (W/unit solid angle)

U_0= radiation intensity of isotropic source (W/unit solid angle)

P_{rad} = total radiated power (W)

For anisotropic source, it is very obvious from (4.11) or (4.12) that the directivity is unity since U, U_{max} and U_0 are all equal to each other. For antennas with orthogonal polarization

components, we define the partial directivity of an antenna for a given polarization in a given direction as “that part of the radiation intensity corresponding to a given polarization divided by the total radiation intensity averaged over all directions.” With this definition for the partial directivity, then in a given direction “the total directivity is the sum of the partial directivities for any two orthogonal polarizations.” For a spherical coordinate system, the total maximum directivity D_0 for the orthogonal θ and φ components of an antenna can be written as

$$D_0 = D_\theta + D_\phi \tag{4.13}$$

While the partial directivities D_θ and D_ϕ are expressed as

$$D_0 = \frac{4\pi U_0}{(P_{rad})_\theta + (P_{rad})_\phi} \tag{4.14}$$

$$D_\phi = \frac{4\pi U_\phi}{(P_{rad})_\theta + (P_{rad})_\phi} \tag{4.15}$$

Where

U_θ = radiation intensity in a given direction contained in θ field component

U_ϕ = radiation intensity in a given direction contained in ϕ field component

$(P_{rad})_\theta$ = radiated power in all directions contained in θ field component

$(P_{rad})_\phi$ = radiated power in all directions contained in ϕ field component

Before proceeding with a more general discussion of directivity, it may be proper at this time to consider another example, compute its directivity, compare it with that of the previous example, and comment on what it actually represents. This may give the reader a better understanding and appreciation of the directivity.

To demonstrate the significance of directivity, let us consider another example in particular let us examine the directivity of a half-wavelength dipole (l = λ/2)

$$D = D_0 \sin^3\theta = 1.67 \sin^3\theta \tag{4.16}$$

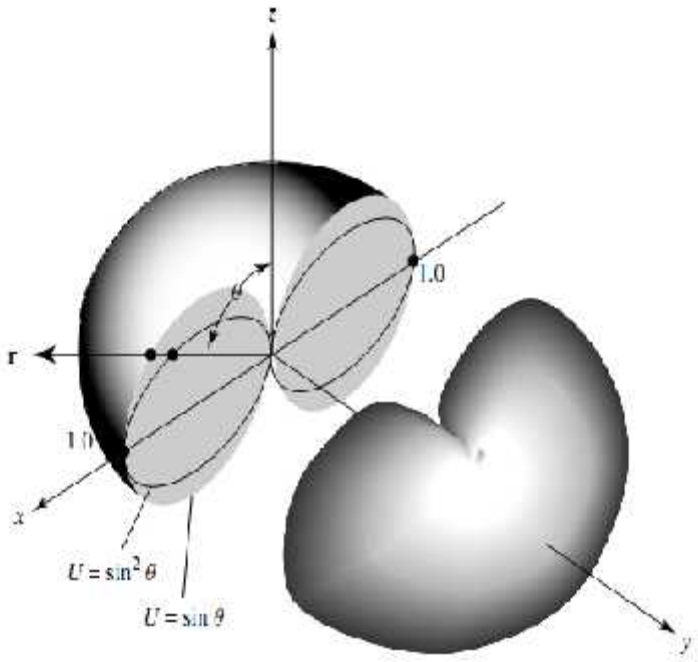

Figure 4.5 Three-dimensional radiation intensity patterns.

Since it can be shown that

$$Sin^3\theta \simeq \left[\frac{Cos(\frac{\pi}{2}cos\theta)}{Sin\theta}\right]^2 \tag{4.17}$$

Where θ is measured from the axis along the length of the dipole. The values represented by (4.16) and those of an isotropic source (D = 1) are plotted two- and three-dimensionally. Let the radiation intensity of an antenna be of the form

$$U = B_0F(\theta,\phi) \simeq \frac{1}{2\eta}\left[\left|E_\theta^0(\theta,\phi)\right|^2 + \left|E_\phi^0(\theta,\phi)\right|^2\right] \tag{4.18}$$

Where B0 is a constant, and E0θ and E0φ are the antenna's far-zone electric-field components. The maximum value of (4.18) is given by

$$U_{max} = B_0F(\theta,\phi)\,|_{max} = B_0F_0(\theta,\phi) \tag{4.19}$$

The total radiated power is found using

$$P_{rad} = \oiint U(\theta,\phi)d\Omega = B_0\int_0^{2\pi}\int_0^{\pi}F(\theta,\phi)\sin\theta d\theta d\phi \tag{4.20}$$

We now write the general expression for the directivity and maximum directivity using (4.11) and (4.12), respectively, as

$$D(\theta,\varphi) = 4\pi \frac{F(\theta,\phi)}{\int_0^{2\pi}\int_0^{\pi} F(\theta,\phi)\sin\theta d\theta d\phi} \tag{4.21}$$

$$D_0 = 4\pi \frac{F(\theta,\phi)|_{max}}{\int_0^{2\pi}\int_0^{\pi} F(\theta,\phi)\sin\theta d\theta d\phi} \tag{4.22}$$

Equation (4.22) can also be written as

$$D_0 = \frac{4\pi}{\left[\int_0^{2\pi}\int_0^{\pi} F(\theta,\phi)\sin\theta d\theta d\phi\right]/F(\theta,\phi)|_{max}} = \frac{4\pi}{\Omega_A} \tag{4.23}$$

Where Ω_A is the beam solid angle, and it is given by

$$\Omega_A = \frac{1}{F(\theta,\phi)|_{max}} \int_0^{2\pi}\int_0^{\pi} F(\theta,\phi)\sin\theta d\theta d\phi = \int_0^{2\pi}\int_0^{\pi} F_n(\theta,\phi)\sin\theta d\theta d\phi \tag{4.24}$$

$$F_n(\theta,\phi) = \frac{F(\theta,\phi)}{F(\theta,\phi)|_{max}} \tag{4.25}$$

Dividing by $F(\theta,\phi)|_{max}$ merely normalizes the radiation intensity $F(\theta,\phi)$, and it makes its maximum value unity. The beam solid angle Ω_A is defined as the solid angle through which all the power of the antenna would flow if its radiation intensity is constant (and equal to the maximum value of U) for all angles within Ω_A.

4.4 Gain

Another useful measure describing the performance of an antenna is the gain. Although the gain of the antenna is closely related to the directivity, it is a measure that takes into account the efficiency of the antenna as well as its directional capabilities. Remember that directivity is a measure that describes only the directional properties of the antenna, and it is therefore controlled only by the pattern. Gain of an antenna (in a given direction) is defined as "the ratio of the intensity, in a given direction, to the radiation intensity that would be obtained if the power accepted by the antenna were radiated isotropically. The radiation intensity corresponding to the isotropically radiated power is equal to the power accepted (input) by the antenna divided by 4π." In equation form this can be expressed as

$$\text{Gain} = 4\pi \frac{\text{radiation intensity}}{\text{total input(accepted) power}} = 4\pi \frac{U(\theta,\phi)}{P_{in}} \quad \text{(dimensionless)} \tag{4.26}$$

In most cases, however, the reference antenna is a lossless isotropic source. Thus

$$G = \frac{4\pi U(\theta,\phi)}{P_{in}\,(lossless\ isotropic\ source)} \qquad \text{(dimensionless)} \tag{4.27}$$

When the direction is not stated, the power gain is usually taken in the direction of maximum radiation. We can write that the total radiated power (P_{rad}) is related to the total input power (P_{in}) by

$$P_{rad} = e_{cd} P_{in} \tag{4.28}$$

Where, e_{cd} = antenna radiation efficiency

Now the definition of two gains one referred to as gain (G), and the other, referred to as absolute gain (G_{abs}), that also takes into account the reflection/mismatch losses

$$G(\theta,\phi) = e_{cd}\left[4\pi\frac{U(\theta,\phi)}{P_{rad}}\right] \tag{4.29}$$

This is related to the directivity by following

$$G(\theta,\phi) = e_{cd} D(\theta,\phi) \tag{4.30}$$

In a similar manner, the maximum value of the gain is related to the maximum directivity then

$$G_0 = G(\theta,\phi)\,|_{max} = e_{cd} D(\theta,\phi)\,|_{max} = e_{cd} D_0 \tag{4.31}$$

Which does take into account the losses of the antenna element itself, it does not take into account the losses when the antenna element is connected to a transmission line, These connection losses are usually referred to as reflections (mismatch) losses, and they are taken into account by introducing a reflection (mismatch) efficiency e_r, which is related to the reflection coefficient $e_r = (1 - |\Gamma|^2)$. Thus, we can introduce an absolute gain Gabs that takes into account the reflection/mismatch losses (due to the connection of the antenna element to the transmission line), and it can be written as

$$G_{abs}(\theta,\phi) = e_r G(\theta,\phi) = (1 - |\Gamma|^2) G(\theta,\phi) = e_r e_{cd} D(\theta,\phi) = e_0 D(\theta,\phi) \tag{4.31}$$

Where e_0 is the overall efficiency as $e_0 = e_r e_c e_d$ and voltage standing wave ratio similarly, the maximum absolute gain G_{abs} of (4.31) is related to the maximum directivity D_0 by

$$G_{0abs} = G_{abs}(\theta,\phi)\,|_{max} = e_r G(\theta,\phi)\,|_{max} = (1 - |\Gamma|^2) G(\theta,\phi)\,|_{max} = e_r e_{cd} D(\theta,\phi)\,|_{max}$$
$$= e_0 D(\theta,\phi)\,|_{max} = e_0 D_0 \tag{4.32}$$

If the antenna is matched to the transmission line, that is, the antenna input impedance Z_{in} is equal to the characteristic impedance Z_c of the line ($|\Gamma| = 0$), then the two gains are equal to ($G_{abs} = G$). The total maximum gain G_0 for the orthogonal θ and φ components of an antenna can be written as

$$G_0 = G_\theta + G_\phi \tag{4.33}$$

While the partial gains G_θ and G_ϕ are expressed as

$$G_\theta = \frac{4\pi U_\theta}{P_{in}} \tag{4.34}$$

$$G_\phi = \frac{4\pi U_\phi}{P_{in}} \tag{4.35}$$

Where

U_θ = Radiation intensity in a given direction contained in E_θ field component

U_ϕ = Radiation intensity in a given direction contained in E_ϕ field component

P_{in} = Total input (accepted) power

Usually the gain is given in terms of decibels instead of the dimensionless quantity of (4.31). The conversion formula is given by

$$G_0(dB) = 10log_{10}[e_{cd}D_0 dimensionsless] \tag{4.36}$$

4.5 ETCSRR Geometric view & Mathematical Modeling

Figure 4.6(a) shows the schematic geometry of an ETCSRR with dimensions indicated. Fig. 4.6(b) shows the equivalent circuit model of the ETCSRR, forming L-C network. The metallic arms of triangle contribute a total inductance, L_m and distributed capacitances C_1 and C_2 forming at the two halves of ETCSRR structure on both sides of the split gaps, g_1 and g_2. The gap capacitance C_{g1} and C_{g2} are due to the splits within the inner and the outer rings respectively. The resonance frequency of the proposed ETCSRR is computed using this equivalent circuit and

the theoretical formulations given in [10] and validated using a commercial CST simulator [11]. The inductance L_m is due to the gap between the rings.

4.5.1 Net Capacitance calculation

When a magnetic field is applied along the z-axis, an electromotive force appears around the ETCSRR which induces a current passing from one arm of triangle to the other through the gaps and the structure behaves like an L-C network having resonant frequency f_0 expressed as:

$$f_0 = \frac{1}{2\pi\sqrt{L_{net}C_{net}}} \tag{4.37}$$

Where L_{net} and C_{net} are the net effective inductance and capacitance of the equivalent L-C network of the ETCSRR.

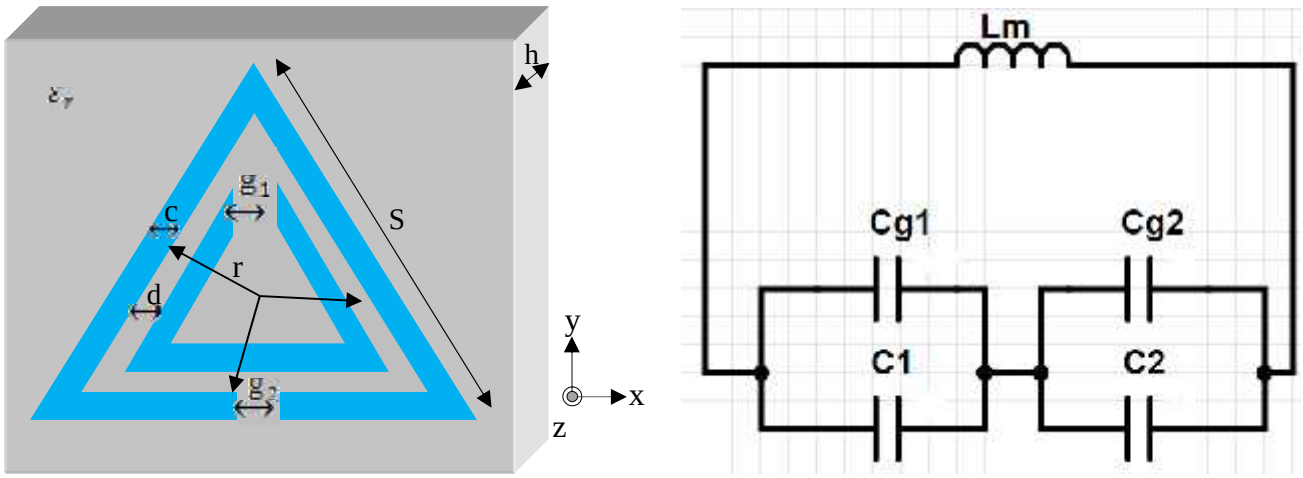

(a) (b)

Fig. 4.6 (a) Schematic geometry of ETCSRR (b) Equivalent circuit of ETCSRR

Considering an axis through the vertical opposite gaps g_1 and g_2 of the ETCSRR and assuming $g_1 = g_2 = g$, it denotes the capacitance of its left and right half arms of the triangle is C_l and C_r. Due to zero skew rotation, C_l must equal C_r and is given by

$$C_{triangle} = C_l = C_r = \left(\frac{p-g}{2}\right).C_{pul} \tag{4.39}$$

Where $p = 3s$ the perimeter of the triangle and C_{pul} is the per-unit-length capacitance of the ETCSRR.

$$C_{pul} = \varepsilon_0.\left(\frac{\varepsilon_r+1}{2}\right).\frac{\varepsilon(\sqrt{1-\sigma^2})}{\varepsilon(\sigma)} \tag{4.40}$$

Where $\upsilon = \frac{d}{d+2c}$ and $\varepsilon(.)$ is the complete elliptical integral of second kind, defined as $\varepsilon(k) = \int_0^{\frac{\pi}{2}} \sqrt{1-(k\sin\theta)^2}\, d\theta$. For an accurate estimation of the resonance frequency, the effect of gap capacitance is also computed using parallel plate capacitance approximation. For $g = g_1 = g_2$, the gap capacitance C_{g1} must equal C_{g2} and is given by

$$C_{gap} = C_{g1} = C_{g2} = \frac{\varepsilon_0.\ \varepsilon_r.C.h}{g} \tag{4.41}$$

Where c is the width of the conductor and h is the depth of the substrate as shown in Fig 4.6(a). Therefore, the net equivalent capacitance of the L-C network, C_{net}, stand out to be

$$\frac{1}{C_{net}} = \frac{1}{(C_1+C_{g1})} + \frac{1}{(C_2+C_{g2})} = \frac{1}{(C_l+C_g)} + \frac{1}{(C_r+C_g)} \tag{4.42}$$

After simplification the net capacitance will be

$$C_{net} = \frac{\beta^2+2\beta C_g+C_g^{\ 2}}{2(\beta+C_g)} \tag{4.43}$$

Where $\beta = \left\{(\frac{p-g}{2})C_{pul}\right\}$ and others defined previously.

4.5.2 Net Inductance calculation

Maxwell showed that the self-inductance of a conducting loop is equal to the mutual inductance between a pair of laments spaced orthogonally apart at a distance termed as the geometric mean distance of the area of the structure. The self-inductance of a wire loop, giving self-inductance as a curve integral is similar to the Neumann formula for mutual inductance. The starting point is

the expression. It can be computed using the general Neumann expression [4]. The starting point is the expression

$$L_s = \frac{\mu_0}{8\pi} \int \frac{j(X) \cdot j(X')}{|X - X'|} d^3x d^3x' \tag{4.44}$$

for the magnetic field energy of a system with current density $\mathbf{j}(\mathbf{x})$, where μ_0 is the magnetic constant.[1] It resembles the expression for gravitational or electrostatic potential energy, the only new ingredient is the scalar product between the current elements. For a current density $j(X) = \sum I_m j_m(X)$ corresponding to N separate current loops with currents I_m and normalized current densities j_m it follows

$$L_s = \frac{\mu_0}{8\pi} \int \frac{j(X) \cdot j(X')}{|X - X'|} d^3x d^3x' = \frac{1}{2} \sum_{m,n=1}^{N} L_{m,n} I_m I_n \tag{4.45}$$

If the currents flow in thin wires, then the integrals become curve integrals, and one immediately reads off the Neumann expression for mutual inductance of two (filamentary) current loops [2]

$$L_{1,2} = \frac{\mu_0}{4\pi} \oint \frac{dX_1 \cdot dX_2}{|X_1 - X_2|} \tag{4.46}$$

It is plausible that there exists a similar expression for the self-inductance of a wire loop. Formally one might read off from equation (4.46) an expression similar to equation (3), where the two closed curves coincide. But this cannot be correct, because $|X - X'|$ now vanishes and the integral isn't defined. Instead we will prove

$$L = \frac{\mu_0}{4\pi} \left(\oint \frac{dX \cdot dX'}{|X - X'|} \right)_{|s - s'| > a/2} + \frac{\mu_0}{4\pi} lY + \cdots \tag{4.47}$$

Where *a* denotes the wire radius and *l* the length of the wire. The variable *s* measures the length along the wire axis. The constant Y depends on the distribution of the current in the cross section of the wire: Y = 0 if the current flows in the wire surface, $Y = 1/2$ when the current is homogeneous across the wire.

The approximation thus is exact in the limit $a \ll l$ except in special cases. The inductance L for a straight segment from equation (4.47) in the appendix thus leads to

$$L = \frac{\mu_0}{4\pi} \left(\oint \frac{dX \cdot dX'}{|X - X'|} \right)_{|s - s'| > b} + \frac{\mu_0 l}{2\pi} \left(\ln\left(\frac{2b}{a}\right) + \frac{Y}{2} \right) + \cdots \tag{4.48}$$

This expression cannot depend on the (more or less) arbitrary length scale *b*, but *b* is the only short length scale in the curve integral.

The curve integral (4.48) for an equilateral triangle with edge length c consists of three times the expression (4.47) for the edges by themselves and three times the interaction energy $L_c(s, s, 120)$ of adjacent edges.

$$L_c = \frac{\mu_0}{2\pi} 3s \left\{ \ln\left(\frac{s}{r}\right) - 1 - ln\frac{3}{2} \right\} \tag{4.49}$$

The table displays the ratio of the exact self-inductance L of an equilateral triangle with border length s and corners with curvature radius r and the curve integral L_c for different border length s,

4.5.3 Physics of SRRs and CSRRs and Its Equivalent-Circuit Models

The analysis of ETCSRRs behaves as a LC resonator that can be excited by an external magnetic flux, exhibiting a strong diamagnetism above their first resonance. ETCSRRs also exhibit cross-polarization effects (magneto electric coupling) [31] so that excitation by a properly polarized time varying external electric field is also possible. Fig. 4.7 shows the basic topology of the ETCSRR, as well as the equivalent-circuit model proposed in [30].

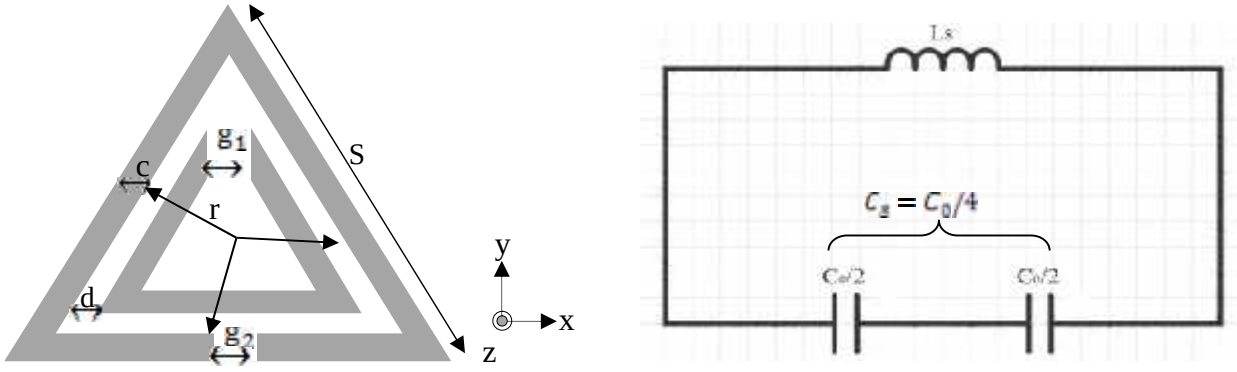

(a) (b)

Fig.4.7 Topologies of the: (a) ETCSRR structure and (b) its equivalent-circuit model

[5

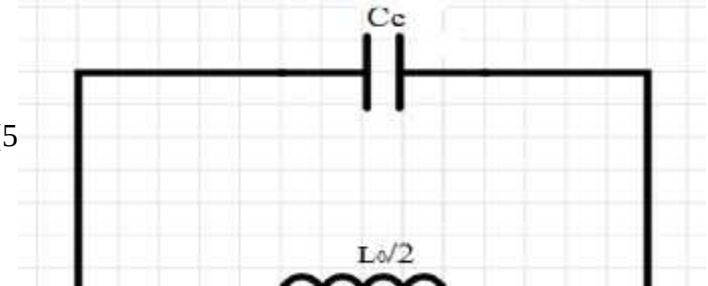

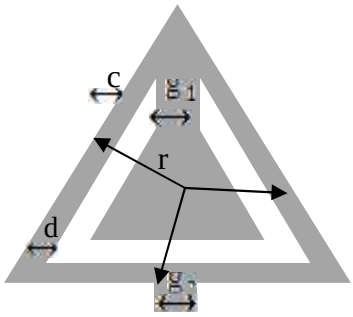

(a) (b)

Fig.4.8 Topologies of the: (a) CETCSRR structure and (b) its equivalent-circuit model (ohmic losses can be taken into account by including a series resistance in the model). Grey zones represent the metallization or patch on substrate.

In this figure, C_0 stands for the total capacitance between the rings, i.e., $C_0 = 3sC_{pul}$ where is C_{pul} the per unit length capacitance between the rings. $f_0 = (L_s C_s)^{-1/2}/2\pi$, where C_s is the series capacitance of the inner and outer ETCSRR, i.e. $C_s = C_0/4$. The inductance L_s can be approximated by that of a single Triangle with averaged radius r and width c [30]. If the effects of the metal thickness and losses, as well as those of the dielectric substrate are neglected, a perfectly dual behavior is expected for the complementary screen of the ETCSRR [28]. Thus, whereas the ETCSRR can be mainly considered as a resonant magnetic dipole that can be excited by an axial magnetic field [30], the CETCSRR (Fig. 4.7) essentially behaves as an electric dipole (with the same frequency of resonance) that can be excited by an axial electric field. In a more rigorous analysis, the cross-polarization effects in the ETCSRR [30], [31] should be considered and also extended to the CETCSRR. Thus, this last element will also exhibit a resonant magnetic polarizability along y -axis (see Fig. 4.7) and, therefore, its main resonance can also be excited by an external magnetic field applied along this direction [28]. These features do not affect the intrinsic circuit model of the elements, although they may affect its excitation model. The intrinsic circuit model for the CETCSRR (dual of the ETCSRR model) is also shown in Fig. 4.7. In this circuit [32], the inductance L_s of the ETCSRR model is substituted by the

capacitance C_e of a triangle of radius $r - C/2$ surrounded by a ground plane at a distance c of its edge. Conversely, the series connection of the two capacitances $C_0/2$ in the ETCSRR model is substituted by the parallel combination of the two inductances connecting the inner disk to the ground. Each inductance is given by $L_0/2$, where $L_0 = 3sL_{pul}$ and L_{pul} is the per unit length inductance of the CPWs connecting the inner disk to the ground. For infinitely thin perfect conducting screens, and in the absence of any dielectric substrate, it directly follows from duality that the parameters of the circuit models for the ETCSRRs and CETCSRRs are related by $C_e = 4(\varepsilon_0/\mu_0)L_s$ and $C_0 = 4(\varepsilon_0/\mu_0)L_0$. The factor of 4 appearing in these relations is deduced from the different symmetry properties of the electric and magnetic fields of both elements, as is sketched in Fig. 4.8. From these relations, it is easily deduced that the frequency of resonance of both structures is the same, as is expected from duality.

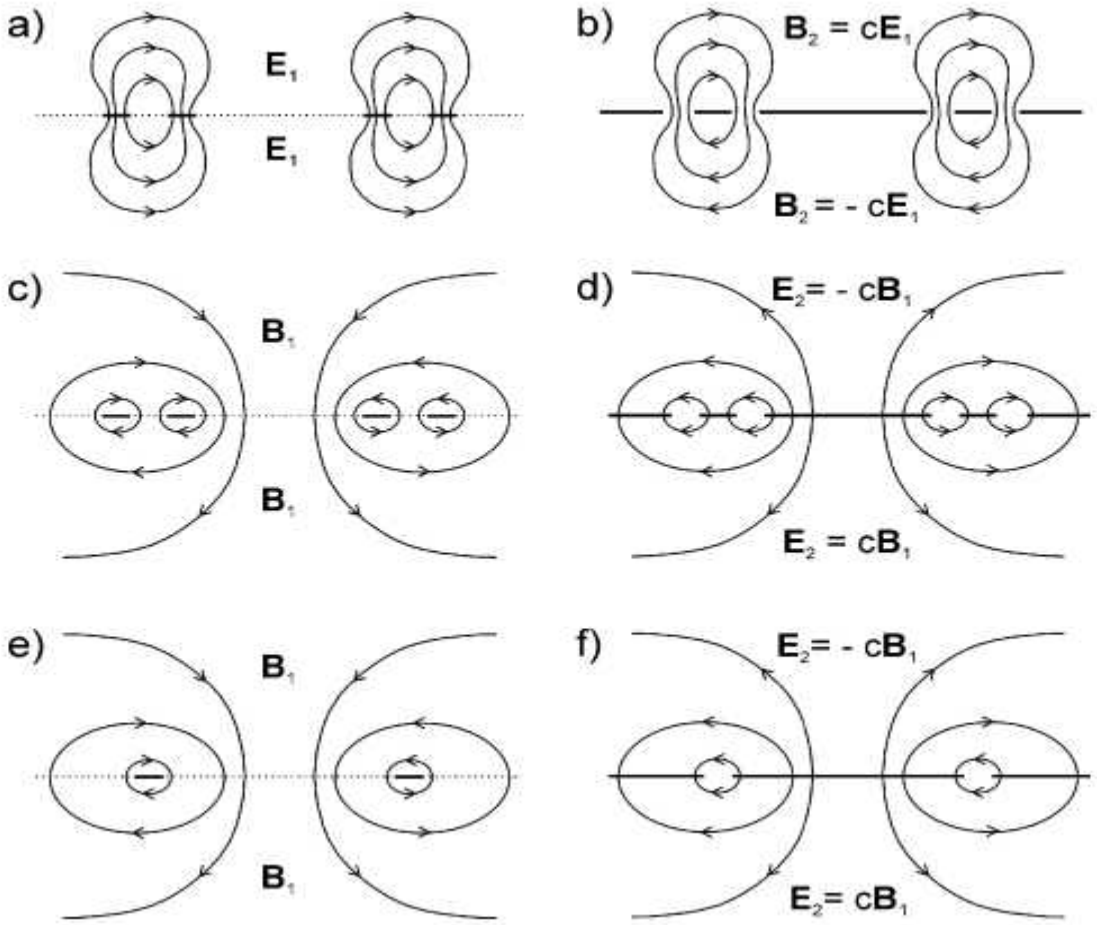

Fig.4.9. Sketch of the electric- and magnetic-field lines in the ETCSRR (left-hand side) and the CETCSRR (right-hand side). (a) Electric-field lines in the ETCSRR at resonance. (b) Magnetic-field lines in the dual CETCSRR. (c) and (d) Magnetic- and electric-field lines in the ETCSRR and CETCSRR, respectively. (e) Magnetic induction field in the equivalent ring inductance used for the computation of L in the ETCSRR [27]. (f) Electric field in the dual equivalent capacitor proposed for the computation of C for the CETCSRR.

CHAPTER 5

Simulation & Results

5.1 Simulation Setup & Results

The software used to model and simulate the microstrip patch antenna is **CST v14.0, Advance Design System (ADS) v15.1** and **Origin Prolab**. The CST analyzes 3D and multilayer structures of general shapes. This is being widely used in RFID application, microwave imaging, patch antenna, designing of waveguide and various kind of RF application. It can be used to calculate and plot the S_{11} parameters, VSWR, radiation pattern, gain, directivity etc. An evaluation version of the software was used to obtain the results for this thesis [22].

5.2 Compare Result

5.2.1 Return Loss

The Return Loss (RL) is a parameter similar to the VSWR to indicate how well the matching between the transmitter and antenna has taken place. It indicates the amount of power that is lost to the load and does not return as a reflection when the transmitter and antenna impedance do not match. Figure 5.1 Show RL of patch antennas with different structures. The f_r has been obtained at 2.443 GHz with RL of -25.83 dB for the conventional patch antenna while it has been shifted to 2.446 GHz with a RL of -28.86 dB due to introducing a resonator cut on patch. The f_r has been shifted because of fringing effect on MPA. Since introduction of a triangular resonator on patch, the RL has been improved; therefore dual resonators with same shape have been presented. For dual triangular cut resonator (DTSRR), the f_r has been obtained at 2.441 GHz with a RL of -33.92 dB. From the chart [23], the RL can be expressed in terms of voltage standing wave ratio (VSWR) which is 1.044:1. The transmitted and reflected powers are 99.95% and 0.05%, respectively with a mismatch loss of 0.002 dB.

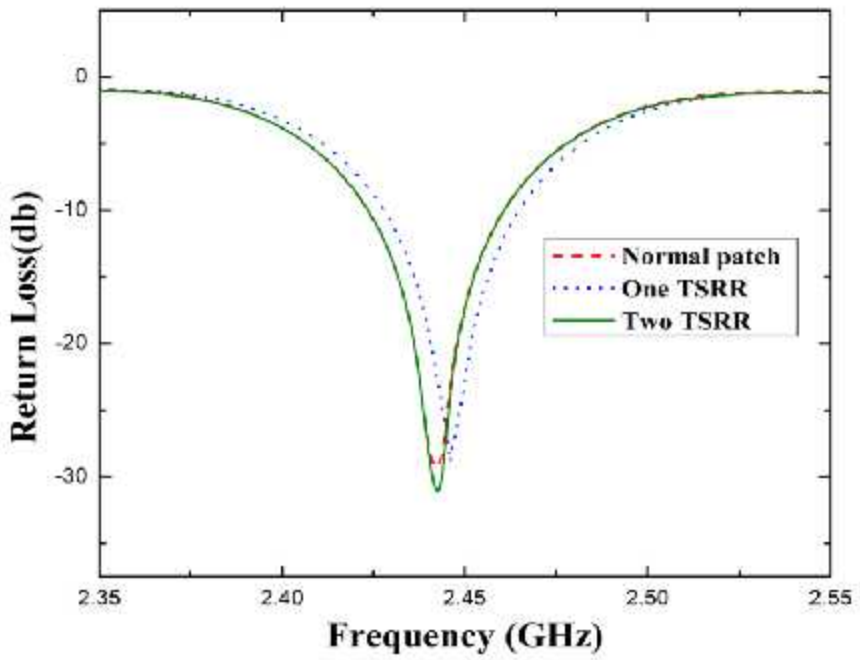

Figure 5.1: Return loss of conventional patch antenna, ETCSRR & proposed DETCSRR

These obtained results are higher than in comparable structures of other resonators [24, 25], thus high gain and high directivity may be expected.

Table 5.1: Simulated results of conventional patch, ETCSRR and DETCSRR antenna

Antenna design	Resonant frequency,f_r (GHz)	Return loss (dB)	Bandwidth (MHz), f_1~f_2 (GHz)	Gain (dB)
Conventional patch	2.443	- 25.835	37.1 (2.4234 ~ 2.4605)	7.72
TSRR	2.446	- 28.864	36.8 (2.4279 ~ 2.4647)	7.85
DTSRR	2.441	- 33.392	37.2 (2.4235 ~ 2.4607)	7.75

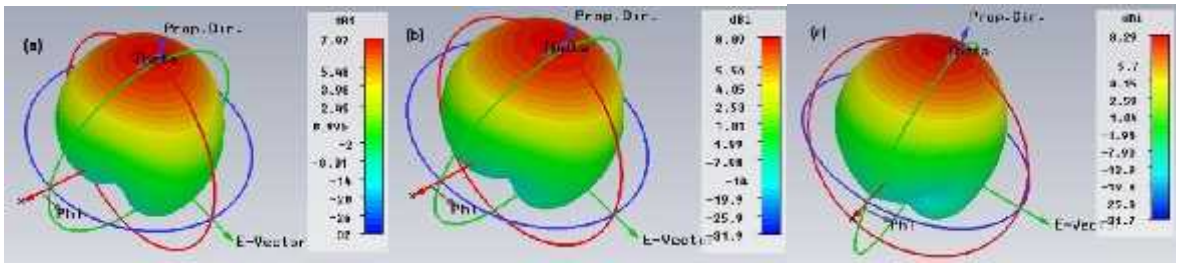

Figure 5.2: The 3D directivity plot of the antenna: (a) conventional patch antenna, (b) ETCSRR antenna, (c) DETCSRR antenna.

From Table 5.1, for conventional patch antenna resonant frequency at 2.443 GHz, 7.72 dB gain has been obtained with a return loss of -25.83 dB. After introducing resonant cut on patch resonant frequency shifts to 2.446 GHz and we have obtained return loss -28.86 dB and gain 7.85 dB. The gain of ETCSRR indicates 7.85 dB which is an improvement of 0.13 dB from conventional antenna gain. Intersecting point of return loss at - 10 dB line of this design has been evaluated for all three antennas for bandwidth calculation. For better performance analysis another triangular shape is introduced on TSRR antenna. Simulated results for DETCSRR at resonant frequency 2.441 GHz return loss of -33.39 dB and gain of 7.75 dB has been obtained. Here proposed triangular loop is a nonmagnetic pure copper metal with gaps in opposite ends. Split gap stores charges and works as a capacitor which accelerates radiation pattern and gain of WLAN antenna. The incorporation of DETCSRR structure has accelerated the antenna performance. These theoretically obtained performances with the introduction of DETCSRR are higher than the previously published values for the conventional split ring resonators [24]. Therefore, we understand that optimization technique in case of dual TSRR can be effective for better antenna performance.

5.2.2 Performance of Proposed Antenna With Respect To Distance between Two ETCSRR Structures

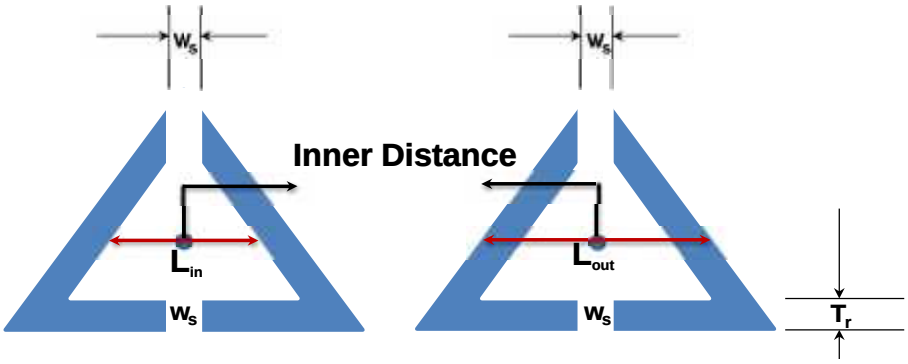

Figure 5.3 Geometric top view of distance between DETCSRR structures

The internal distance between two TSRR has also been analyzed for T_r = 1 mm. When inner distance is 9.02 mm, the best RL is -37.990 dB whereas a high gain of 7.75 dB is achieved for 8.02 mm. The gain has started to decrease for above the inner distance of 9.02 mm. Calculated bandwidths are found similar for all cases. Therefore, the optimized parameters are T_r = 1 mm and inner distance = 9.02 mm for the DETCSRR to achieve high performance.

Table 5.2: Simulated results of distance between two DETCSRR structures for t_r = 1 mm

Distance between two TSRR structure (mm)	Resonant frequency, f_r (GHz)	Return loss (dB)	Bandwidth (MHz), f_1 ~ f_2 (GHz)	Gain (dB)
7.50	2.442	-32.308	37.4 (2.4232 ~ 2.4606)	7.75
8.02	2.447	- 33.392	37.2 (2.4235 ~ 2.4607)	7.75
9.02	2.441	- 37.990	37.6 (2.4236 ~ 2.4612)	7.73
12	2.443	- 35.922	37.5 (2.4235 ~ 2.461)	7.71
15	2.442	- 34.345	37.5 (2.4233 ~ 2.4608)	7.70

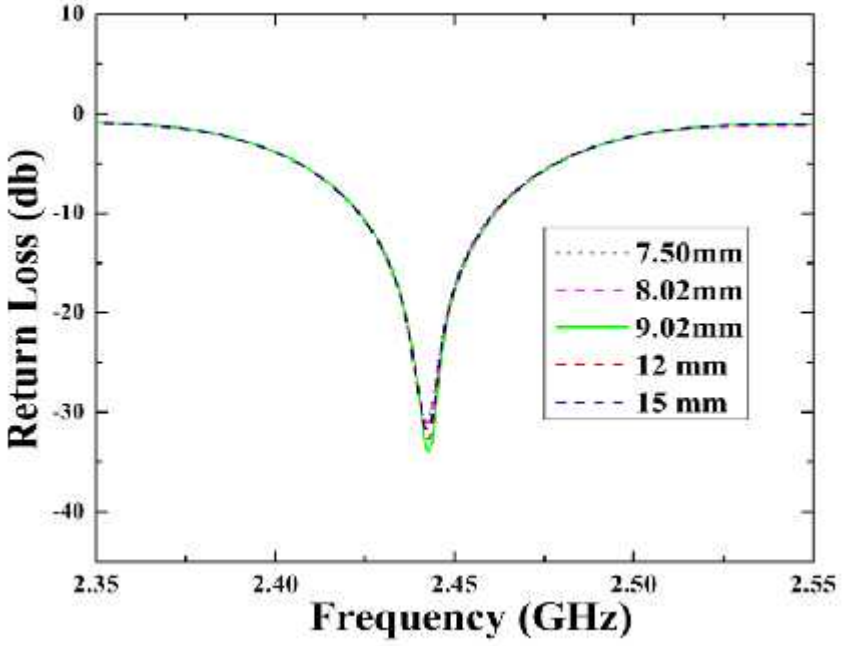

Figure 5.4: The return loss of patch antenna with different distance between two ETCSRRs structure.

5.2.3 Performance of Proposed Antenna with Respect Size of ETCSRR Structure

In this phase of optimization process, the performance of DETCSRR antenna has been investigated with respect to resonator's size (width of cut resonator, T_r). The results have been showed in table 4.4. Among five different T_r, the best RL and the highest gain have been observed as -33.392 dB and 7.94 dB, respectively.

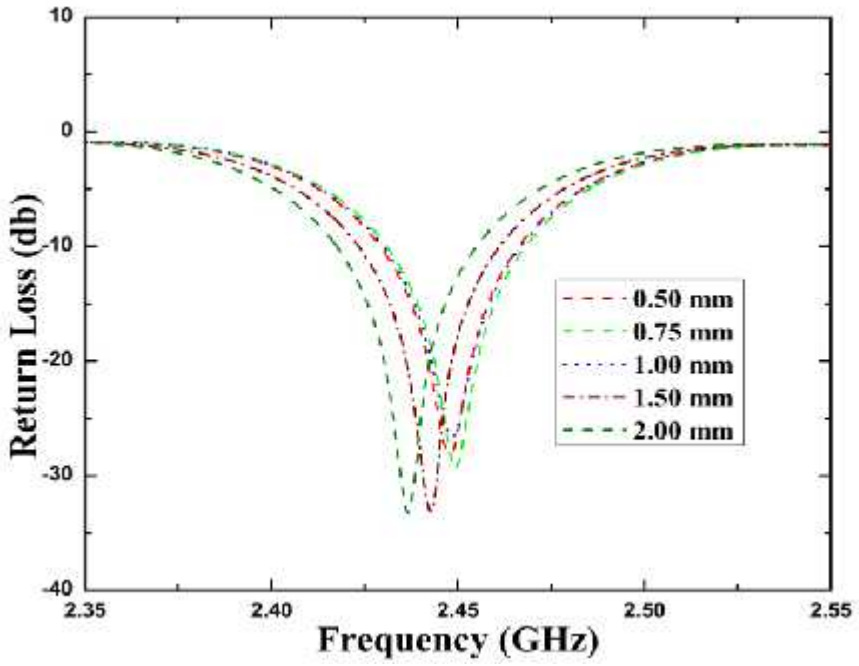

Figure 5.5: The return loss of patch antenna with different size of ETCSRR structure.

Table 5.3: Simulated results of DETCSRR antenna with different t_r size

Size of TSRR T_r(mm)	Resonant frequency, *fr* (GHz)	Return loss (dB)	Bandwidth (MHz), f_1 ~ f_2 (GHz)	Gain (dB)
0.50	2.443	-28.849	37.1 (2.4281 ~ 2.4652)	7.88
0.75	2.446	-31.638	37.2 (2.4235 ~ 2.4607)	7.94
1.00	2.441	- 33.392	37.5 (2.4139 ~ 2. 4514)	7.75
1.50	2.445	- 30.228	36.8 (2.4016 ~ 2.4384)	7.51
2.00	2.449	- 27.353	37.1 (2.4281 ~ 2.4652)	7.60

5.2.4 Performance of Proposed Antenna With Respect To Increment Number of ETCSRRs Structure

Antenna gain is a parameter which is closely related to the directivity of the antenna. The gain of patch antennas has been the goal of many researchers [26]. Table 5.4 describes the various antenna parameters with respect to the number of triangular resonators.

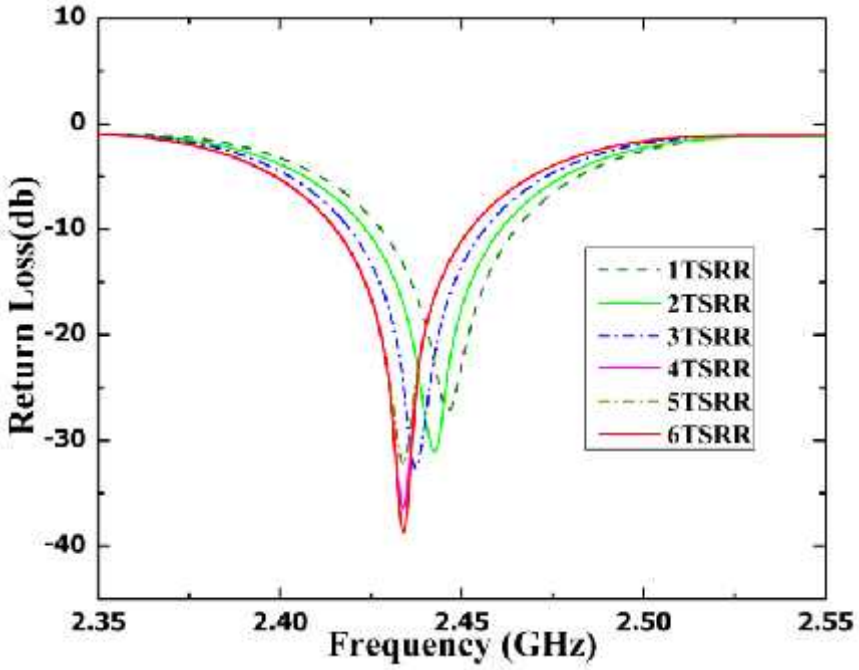

Figure 5.6: Return loss of patch antenna with respect to increment number of ETCSRR Structure

Table 5.4: Return loss of patch antenna with increment number of ETCSRR row wise alignment

No of TSRR	Resonant frequency, *fr* (GHz)	Return loss (dB)	Directivity(dBi)	Gain (dB)
One TSRR	2.446	- 28.864	8.29	7.85
Two TSRR	2.443	- 33.392	8.25	7.75
Three TSRR	2.437	- 36.118	8.21	7.32
Four TSRR	2.434	- 41.765	8.30	7.34
Five TSRR	2.434	-35.82	8.31	7.33
Six TSRR	2.434	-29.694	8.24	7.35

This may be due to addition of capacitive charge concentration across width of MPA. So, incorporation of CTSRR on MPA can be utilized as frequency shifter.

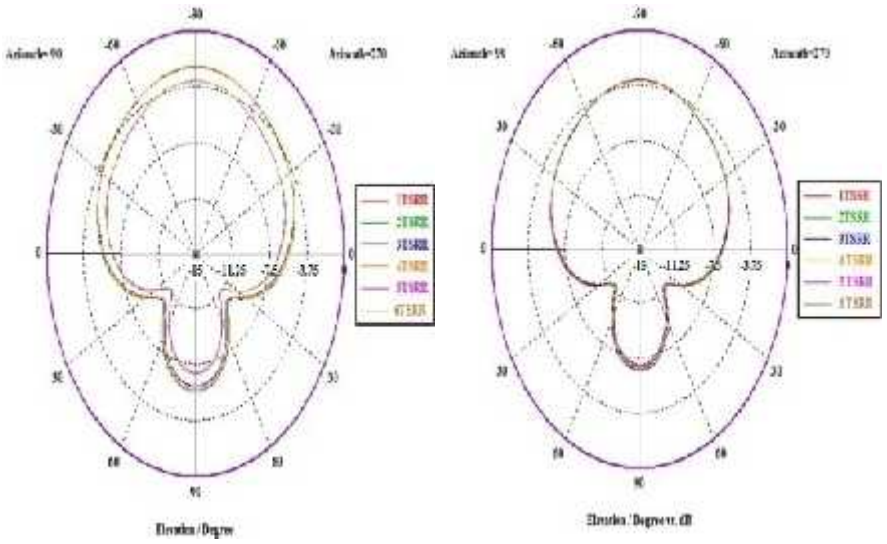

Fig. 5.7: Fairfield gain and directivity of patch antenna with respect to increment of TSRR.

It has been observed that highest gain is achieved on antenna with one CTSRR and most directivity is achieved on antenna with five CTSRR. But on the other hand, return loss improves with respect to increment of CTSRR on patch and interestingly this shift to lower frequency region.

5.2.5 Performance of Proposed Antenna With Respect To Orientation of ETCSRR Structure

Figure 5.8 shows the variation pattern of dual units of triangular SRR. In this work, ten different of T-SRR variation pattern had been simulated to compare the return loss and gain performance between the normal patch antenna and triangular SRR patch antenna.

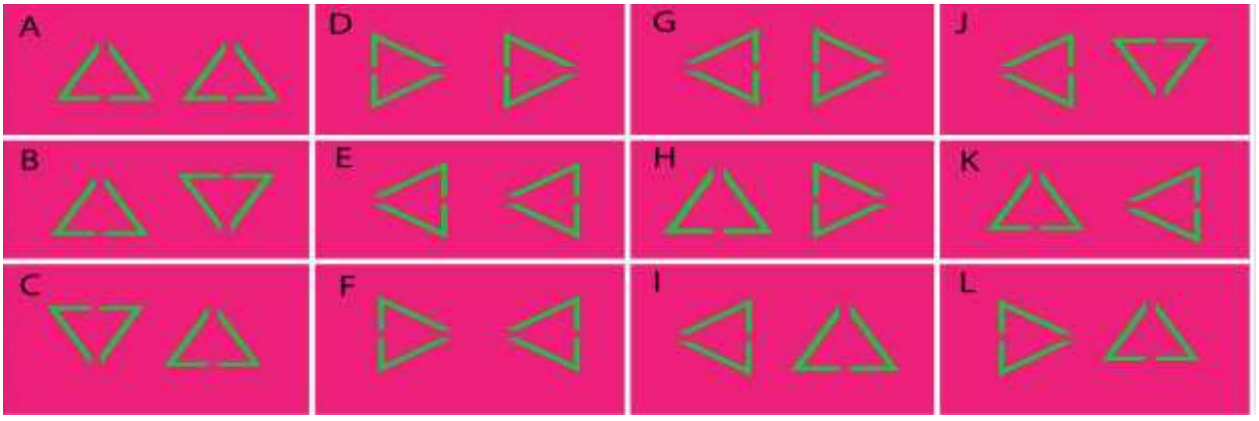

Figure 5.8: The variation pattern of double units of ETCSRR – Pattern A to Pattern L.

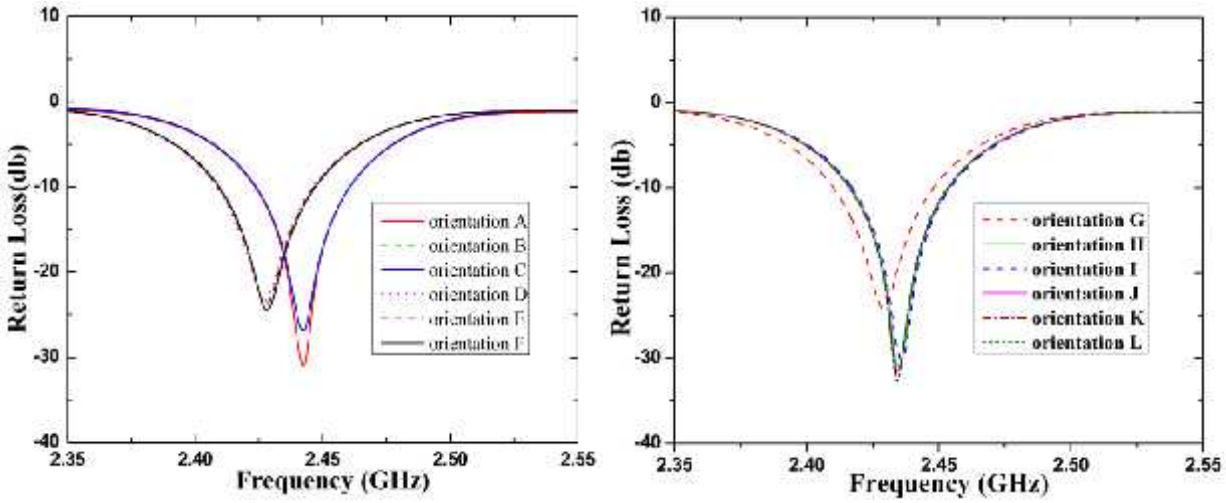

(a) (b)

Figure 5.9: (a) The return loss of patch antenna F to pattern J. (b) The return loss of patch antenna G to pattern L.

Different variation pattern also effects the performance of the patch antenna. From the Figure 5.9 (a) and (b) and Table 5.5, it shows that pattern A and pattern B give the best gain result with 7.75dB and 7.73dB while the worst had been shown by pattern D, E and pattern F with only 7.39 dB and 7.40 dB respectly. All SRR pattern shows the approximatly same resonant frequency and directivity that is 2.434 GHz and 8.28 dBi. From the table, it shows that the best return loss is shown by pattern L with - 36.084dB compare with Pattern K with only – 35.125dB. Another ten patterns are considered that were pattern A, pattern B, pattern C, pattern D, pattern E, pattern F, pattern G, pattern H, pattern I and pattern J shown in Figure 5.8. The higher gain performance had been shown by pattern A with 7.75 dB while the worst gain performance had been shown by pattern D and pattern F with only 7.39 dB and 7.40 dB.

These entire four patterns show the same resonant frequency result that is in 2.434GHz but it located different with the pattern A, pattern B, pattern C, and pattern D. Pattern L achieved the best return loss performance with 36.084 dB followed by pattern J and pattern K with -34.127 dB and -35.125 dB.

The worst return loss had been shown by pattern D with only - 23.968dB. So, for a conclusion different variation pattern did not effect the too much about gain and directivity but only shifted frequency into the new resonant point. The proposed antenna design can be integrated with RF transmitter [27] and R receiver [28] to form a complete WLAN front-end system.

Table 5.5: The return loss of patch antenna for different DETSRR pattern A to pattern L

TSRR Orientation	Resonant frequency, f_r (GHz)	Return loss (dB)	Gain (dB)	Directivity(dBi)
A	2.443	- 33.391	7.75	8.11
B	2.443	- 28.245	7.73	8.10
C	2.443	- 28.175	7.73	8.21
D	2.428	- 23.968	7.39	8.29
E	2.428	-24.727	7.40	8.16
F	2.428	- 25.449	7.39	8.16
G	2.428	- 24.790	7.41	8.25
H	2.434	- 32.747	7.56	8.27
I	2.437	- 31.636	7.57	8.29
J	2.434	-34.127	7.56	8.28
K	2.434	-35.125	7.55	8.13
L	2.433	-36.084	7.56	8.13

5.3 Velidefication of Proposed Structure

In this section proposed structure and its equivalent circuit is deducted and represent the equality of performance parameter full structure with its equivalent circuit model by using CST and ADS software.

5.3.1 Proposed Structure and its Equivalent circuit Model

The proposed structure of CTSRR is newly designed with strip width c and spacing g1 and g2 between the divided parts of triangle. The equivalent circuit model of the CTSRR is presented in Fig. 5.10 (b), which behaves as a resonant cavity modeled by an LC circuit. The inductance is due to the gap between the two halves of CTSRR and the capacitance is due to the gaps in the rings itself. The divided pure copper part of triangle contributes inductances L_1, L_2 and Cg1,

Cg2 are the gap capacitances due to the triangular splits within the upper and the bottom part respectively. Here, magnetic field H, perpendicular to the plane, allows the creation of gaps capacitance at the opening of the ring.

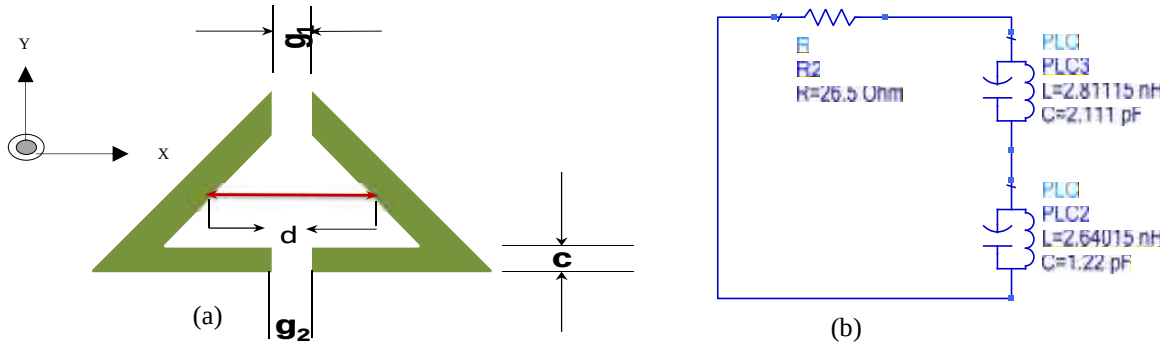

Figure 5.10: (a) Proposed structure. (b) The Equivalent circuit of proposed structure.

5.3.2 Complete Antenna with Proposed Structure and its Equivalent circuit Model

The complete structure is constructed by putting on proposed structure on patch and its equivalent circuit is derivation.

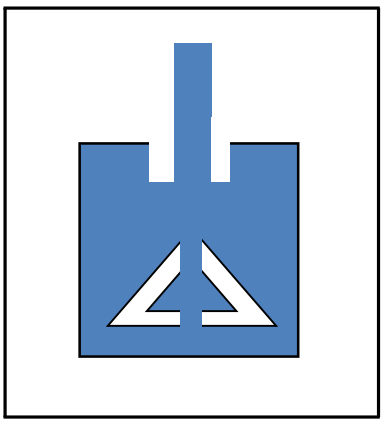

Figure 5.11: Antenna with proposed structure or complete design.

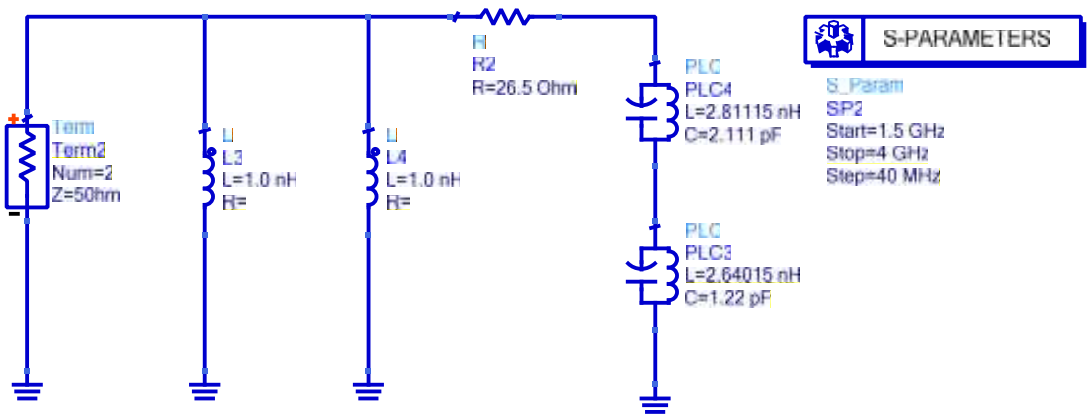

Figure 5.12: Complete Equivalent circuit Model with respect to above figure (Fig.5.11).

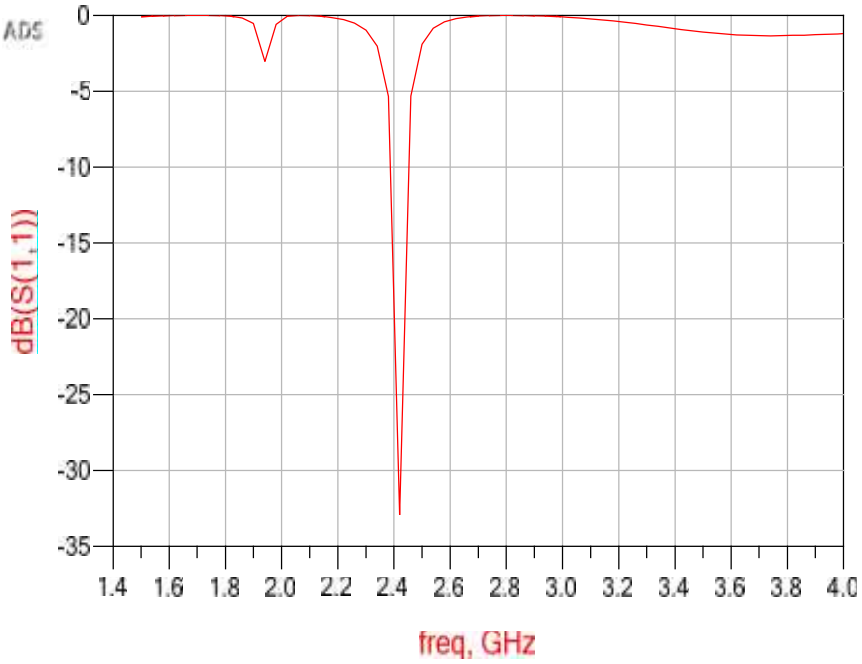

Figure 5.13: Return Loss from one ETCSRR equivalent circuit using ADS

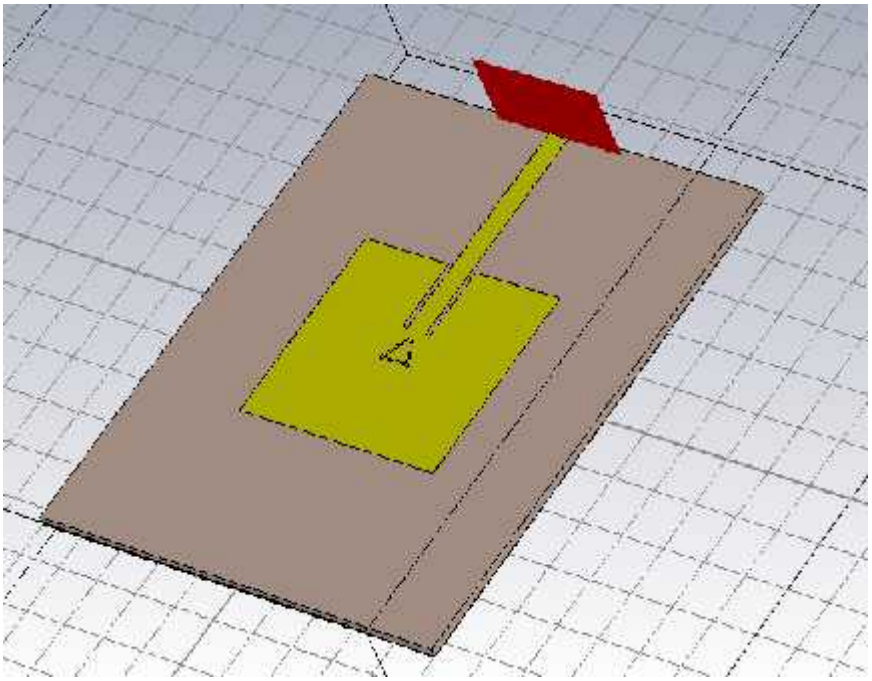

Figure 5.14: Antenna with single ETCSRR with CST software image

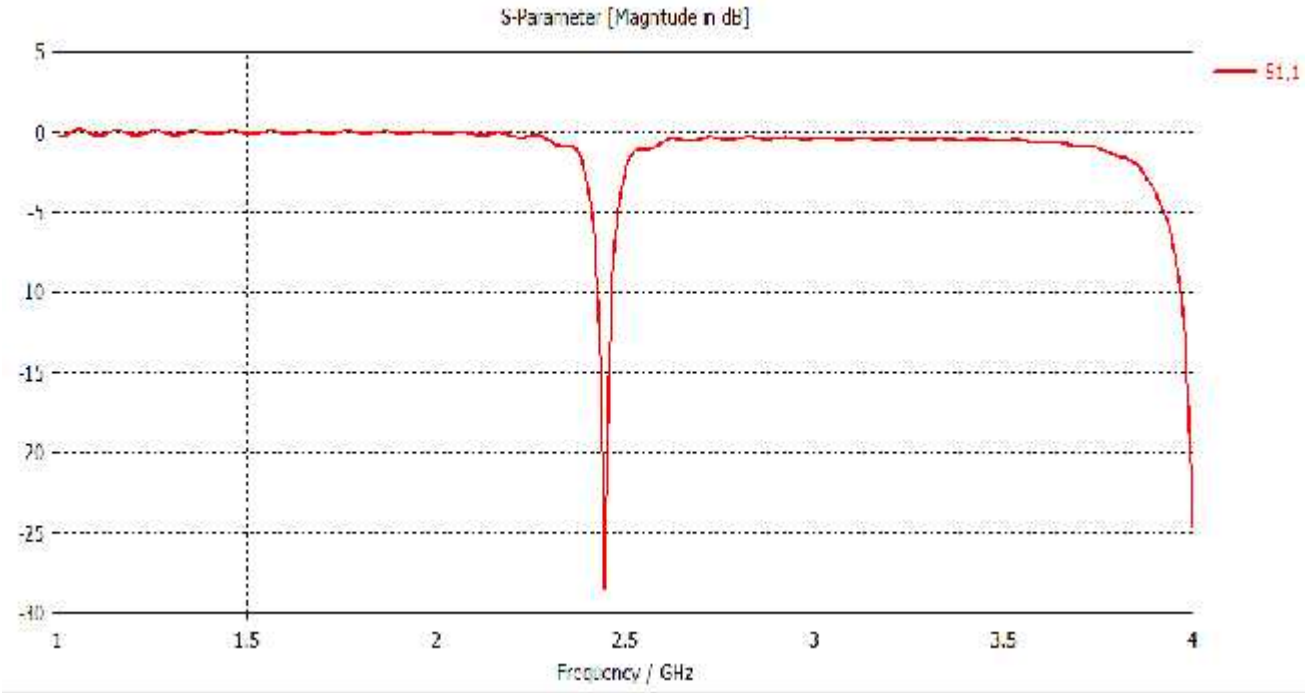

Figure 5.15: Return Loss from Antenna with one ETCSRR using CST

5.3.3 Comparison of Return Loss of Patch Antenna and Equivalent circuit

The following graph represents the comparison of return loss of complete structure with its equivalent circuit. It shows the return loss of both graphs approximately same. So it is clearly established that equivalent circuit of proposed structure truly match.

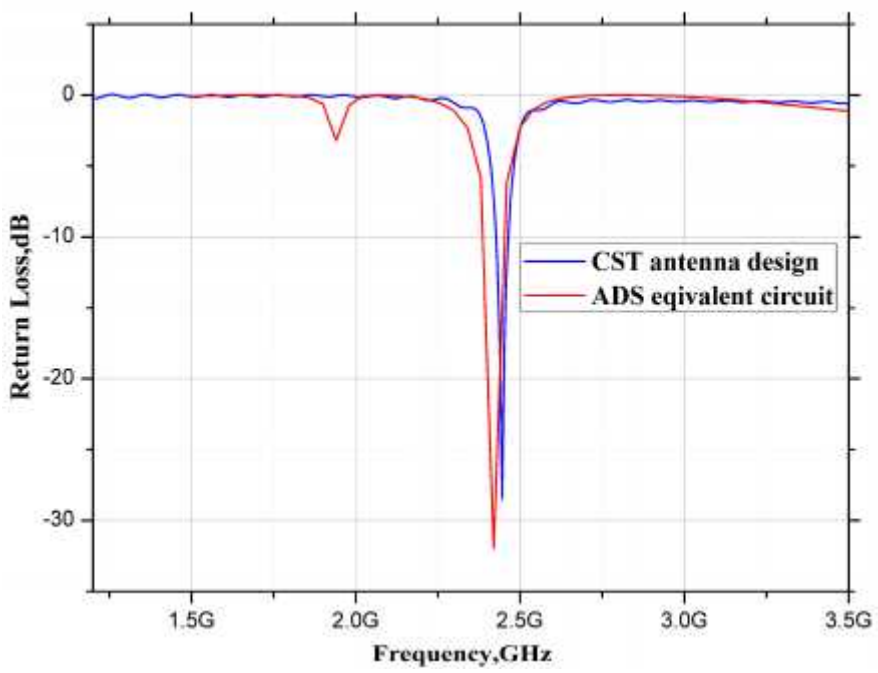

Figure 5.16: Return Loss from one ETCSRR equivalent circuit using ADS

CHAPTER 6

Conclusion

6.1 Introduction

This thesis has focused on the optimization of the performance parameter of the patch antenna using single ETCSRR and DETCSRR structure. The practical implementations of DETCSRR structure microwave devices are still immature. In order to achieve the progress and applicability of ETCSRR and DETCSRR structure rectangular patch antenna, detailed device simulation is necessary. In this work, we have theoretically designed patch antenna by using single ETCSRR and DETCSRR structure micsrostrip patch antenna. The performances of the proposed patch antenna have been evaluated using CST v14.0 and Origin Prolab. These include the theoretical analysis and calculation of input impedance, return loss, radiation pattern, directivity, gain, and efficiency.

6.2 Result

The impact of CETCSRR on the performance of microstrip patch antenna is theoretically investigated. For various orientation of CETCSRR and increment of CETCSRR unit cell, the antenna resonates between 2.43 to 2.45 GHz bands. The antenna shows a directional radiation pattern and capacitive charge develops in gap-cut position improves gain and directivity. Numerical study of the effect and physical parameters of CETCSRR on antenna has been carried out. Resonance frequency shifts toward the lower frequency region with the increment of CETCSRR unit cell. So, proposed design may be helpful for frequency tunable solution. Expected improvement in bandwidth has not been observed due to patch antenna feeding technique. Table 6.1 summaries the results that we have found from our work and compared it with the microstrip patch antenna with different SRR structure results.

Table 6.1: Comparisons between result of proposed antenna and some recent years work using different SRR

Researcher, year	SRR structure type	Application SRR	Size (mm)	Frequency (GHz)	Return loss (dB)	Gain (dBi)
Huda, 2008 [29]	Square edge-couple SRR with 2 ring gap	Microstrip antenna	9.1 x 9.1	2.4	- 18	7.47
Zhang, 2009 [30]	Square edge couple SRR	Circular/dual polarization antenna	5.8 x 5.8	4.37	> - 15	> 5.4
Rahim, 2009 [31]	Square edge-couple SRR with 2 ring gap	Microstrip antenna	49 x 17. 2	2.7	> - 10	11.08
Zani, 2010 [32]	Square edge couple SRR	Circular patch antenna	20 x 20	4.7	- 24.2	1.99
Jiun-Peng, 2011 [33]	Edge-coupled SRR S	Slot dipole antenna	6 x 6 2	2.49	> - 25 4	4.71
Ortiz,2011 [34]	Complementary edge-couple SRR	Dual band patch antenna	4.6 x 4.2 4	4.19, 4.81	> - 20, > - 10	5.95, 5.85
Xiaoyu, 2011[35]	Complementary rectangular edge couple SRR	Folded patch antenna	15 x 7.3	2.36	- 18.4	0.1
Proposed ETCSRR	Equilateral Triangular cut SRR	Rectangular Microstrip patch antenna	48.60 x 41.73	2.44	-28.864	7.87
Proposed DETCSRR	Equilateral Triangular cut SRR	Rectangular Microstrip patch antenna	48.60 x 41.73	2.44	-33.392	7.75

6.3 Conclusion

The above compared results indicate that the proposed ETCSRR and DETCSRR structure rectangular patch antenna is very promising for the wireless application especially in WLAN Application due to high gain and directivity. As there are few limitations like, expected improvement in bandwidth has not been observed due to patch antenna feeding technique. In future, various structural modifications in an optimized way can be a solution for better performance and allow investigating bandwidth enhancement.

6.4 Future Works

The research described in this thesis was concerned with the theoretically designed ETCSRR and DETCSRR structure patch antenna. The proposed antenna has been successfully designed with many exciting results. These have created the way for future work with a goal to fabricate practical ETCSRR and DETCSRR structural high performance patch antenna. There are many areas where further work is required. The works remaining for future study are discussed as follows. The bandwidth limitations of the designed antenna can be improved by employing aperture coupled feeding technique or stacked patch configuration. Also in future, various structural modifications in an optimized way can be a solution for better performance and allow investigating bandwidth enhancement. Surface waves responsible for reducing the performance of the designed antenna can be improved by using substrates or ground planes with photonic band-gaps. A WLAN antenna needs to be versatile and perform without prior alignment in order to reach the optimum throughput. This attribute of the antennas will be ideal for WLAN applications.

REFERENCES

[1] P. Rastogi and K. Cecil, "S and C Bands Multilayer T-Slot Photonic Band gap Micro Strip Antenna", *IOSR Journal of Engineering*, vol. 2, no. 4, pp. 773–776, 2012.

[2] R. J. Chitra, "Design of Double L-slot Microstrip Path for WiMAX and WLAN Application", *Science and Technology (CREST) Journals*, vol. 2, pp. 2–5, 2012.

[3] B. Mazumdar and W. Bengal, "A Compact Printed Antenna For WiMAX , WLAN & C Band Applications", *International Journal Of Computational Engineering Research,* vol. 2, no. 4, pp. 1035–1037, 2012.

[4] C. Jung and F. De Flaviis, "A Dual-Band Antenna for WLAN Applications by Double Rectangular Patch with 4-Bridges", pp. 4–7.

[5] H. Sabri and Z. Atlasbaf, "WLAN APPLICATIONS", *Progress In Electromagnetics Research Letters,* vol. 5, pp. 87–98, 2008.

[6] S. Tignath, L. Shrivastava and D. Sharma, "Triple Band Square Patch Antenna", Science and Technology (CREST) Journals, vol. 01, no. 02, pp. 45–49, 2013.

[7] A. Das and B. Datta, "Multi-Band Microstrip Slotted Patch Antenna for Application in Microwave Communication*", International Journal of Science and Advanced Technology,* vol. 2, no. 9, pp. 91–95, 2012.

[8] Thread-microstrip-patch-antenna-full-report.

[9] Z. N. Chen, Antennas for Portable Devices, John Wiley & Sons, Ltd, 2007.

[10] S. Y. Liao, Microwave Devices and Circuits, 3rd edition.

[11] K. D. Prasad, Antenna and Wave Propagation, Satya Prakashan, New Delhi, 2005

[12] Z. Nasimuddin and N. Chen, Wideband Microstrip Antennas with Sandwich Substrate, Institute for Information and communication Research, 20 Science Park Road, Singapore.

[13] John L. Volakis, The Antenna Engineering Handbook, McGraw-Hill, p. 36-5, 2007.

[14] J R James and P S Hall, Handbook of Microstrip Antennas volume 1 and 2, Pete Peregrinus Ltd, pp. 871-906, 1989.

[15] D. B. Juan, B. Jordi, M. Ferran, M. S. Ricard, "Equivalent-Circuit Models for Split-Ring Resonators and Complementary Split-Ring Resonators Coupled to Planar Transmission

Lines", *IEEE transactions on microwave theory and techniques,* vol. 53, no. 4, pp. 1451-1461, April 2005.

[16] G. B. Philippe and J. F. Olivier, "Electromagnetic resonances in individual and coupled split-ring resonators," *Journal of applied physics,* vol. 92, no. 5, pp. 2929-2936, Sept. 2002.

[17] F. Medina, R. Marques, J. Martel and F. Mesa, "Left-Handed-Media Simulation and Transmission of EM Waves in Sub wavelength Split-Ring-Resonator-Loaded Metallic Waveguides", *Physical review letters*, vol. 89, no.18, pp. 3901-3904,October 2002.

[18] E. Özbay, and K. B. Alici, "Radiation properties of a split ring resonator and monopole composite," *Physics and Statistics Solution*, vol. 244, no. 4, pp. 1192–1196, 2007.

[19] K. Aydin, K. Guven, M. Kafesaki, L. Zhang, C. M. Soukoulis, and E. Ozbay, "Experimental observation of true left-handed transmission peak in metamaterials", *Opt. Lett.*, vol. 29, pp. 2623-2625, 2004.

[20] M. Kara, "The Calculation of the Input Resistance of Rectangular Microstrip Antanna Elements with Various Substrate Thicknesses", *Microwave and Optical Technology Letter,* vol. 13, pp. 137-142, 1996.

[21] P. S. Nakar, "Design of a Compact Microstrip Patch Antenna for use in Wireless/Cellular Devices, Master of Science's thesis", *Dept. of Electrical and Computer Engineering,* Florida State University, USA, 2004.

[22] H. Nornikman, B.H. Ahmad, M.Z.A. A. Aziz, F. Malek, H. Imran and A.R. Othman, "Study and Simulation of an Edge Couple Split Ring Resonator Absorber", Progress In Electromagnetics Research, pp.10, 2012.

[23] Return loss to VSWR conversion table Marki Microwave, [Online]: http://www.markimicrowave.com/Assets/data/return%20loss%20to%20vswr.pdf M. Gil, J.

[24] Patel, S. S. and Y. P. Kosta, "Multiband PBG Suspended Patch Antenna", 2011 *3rd International Conferences on Electronics Computer Technology (ICECT)*, Kanyakumari, India, pp. 5-9, 2011.

[25] H. Nornikman, B. H. Ahmad, A. Aziz and A. R. Othman, "Effect of Single Complimentary Split Ring Resonator Structure on Microstrip Patch Antenna Design", *IEEE Symposium on Wireless Technology and Applications (ISWTA),* pp. 239-244, September, 2012.

[26] F. Bilotti, A. Toscano, L. Vegni, K. Aydin, K. B. Alici and E. Ozbay, "Equivalent-Circuit Models for the Design of Metamaterials Based on Artificial Magnetic Inclusions", *IEEE*

Transactions on Microwave Theory and Techniques, vol. 55, no. 12, pp. 2865-2873, 2007.

[27] N. A. Shairi, T. Abd Rahman and M. A. Aziz, "RF Transmitter System Design for Wireless Local Area Network Bridge at 5725 to 5825 MHz", *International Conference on Computer and Communication Engineering (ICCE 2008)*, pp. 109-112, 2008.

[28] N. A. Shairi, T. A. Rahman, M. Z. and A. Aziz, "RF Receiver System Design For Wireless Local Area Network Bridge at 5725 to 5825 MHz", *Asia Pacific Conference on Applied Electromagnetics (APACE 2007)*, pp. 1-6, 2007.

[29] M. Gil, J. Bonache and F. Martin, "Metamaterial Filters: A Review, Metamaterial", vol. 2, pp. 186-197, 2008.

[30] Z. Hui, L. You-Quan, C. Xi., F. Yun-Qi and Y. Nai-Chang, "Design of Circular / Dual – Frequency Linear Polarization Antennas Based on the Anisotropic Complementary Split Ring Resonator", *IEEE Transaction on Antenna and Propagation,* vol. 57, Issue 10, Part 2, pp. 335 –3355, 2009.

[31] M. K. A. Rahim, H. A. Majid and T. Masri, "Microstrip Antenna Incorporated with Left-Handed Metamaterial at 2.7 GHz", *IEEE International Workshop on Antenna Technology (iWAT 2009),* pp. 1-4, 2009.

[32] M. Z. M. Zani, M. H. Jusoh, A. A. Sulaiman, N. H. Baba, R. A. Awang and M. F. Ain, "Circular Patch Antenna on Metamaterial", *International Conference on Electronic Devices, Systems and Applications (ICEDSA),* pp. 313–316, 2010.

[33] C. Jiun-Peng, and H. Powen, "A Miniaturized Slot Dipole Antenna Capacitively Fed by a CPW with Split Ring Resonators", *IEEE International Symposium on Antennas and Propagation (APSURSI),* pp. 779-781, 2011.

[34] Ortiz N., F. Falcone and M. Sorolla, "Radiation Efficiency Improvement of Dual Band Patch Antenna Based on a Complementary Rectangular Split Ring Resonator", 5th European Conference on Antennas and Propagation (EUCAP), pp. 830-834, 2011.

[35] Xiaoyu C., S. Jun, K. Cheolbok, D. E. Senior and Y. Yong-Kyu, "A Compact Self Packaged Patch Antenna with Non-Planar Complimentary Split Ring Resonator Loading", *IEEE International Symposium on Antennas and Propagation (APSURSI),* pp. 1036 – 1039, 2011.